J|A|C|S
ARTICLES
Published on Web 04/30/2004

Transformation of Acyclic Alkenes to Hydrido Carbynes by (PNP^R)Re Complexes

Oleg V. Ozerov,† Lori A. Watson, Maren Pink, and Kenneth G. Caulton*

Contribution from the Department of Chemistry, Indiana University, Bloomington, Indiana 47405

Received December 10, 2003; E-mail: caulton@indiana.edu

Abstract: Synthesis of (PNP^R)ReOCl$_2$ (PNP^R = (R$_2$PCH$_2$SiMe$_2$)$_2$N, R = ^{i}Pr, Cy, and ^{t}Bu) from (Me$_2$S)$_2$ReOCl$_3$ and (PNP^R)MgCl is described. Magnesium and H$_2$ convert (PNP^R)ReOCl$_2$ first to (PNP^R)ReO(H)$_2$ and then to (PNP^R)Re(H)$_4$, the last being an operationally unsaturated species which can bind PMe$_3$ or *p*-toluidine. Acyclic alkenes react with (PNP^R)Re(H)$_4$ at 22 °C to give first (PNP^R)Re(H)$_2$(olefin) and then (PNP^R)ReH(carbyne), in equilibrium with its η^2-olefin adduct. Re can also migrate to the terminal carbon of internal olefins to form a carbyne complex. Allylic C−SiMe$_3$ or C−NH$_2$ bonds are not broken, but OEt, OPh, and F vinyl substituents (X) are ultimately cleaved from carbon to give the Re≡C−CH$_3$ complex and liberate HX. DFT calculations, together with detection of intermediates for certain olefins, help to define a mechanism for these conversions.

Introduction

The chemistry of the fragment RuHClL$_2$ (L = P^{i}Pr$_3$), which exists as the chloride-bridged dimer[1] [RuH(μ-Cl)L$_2$]$_2$ but gives monomeric products with Lewis bases and olefins, is satisfactorily rationalized as being a π-electron rich species "in search of" π-acid ligands. Of special interest, it has the kinetic and thermodynamic ability to isomerize certain olefins to carbene and even carbyne ligands.[1−13] This characteristic reactivity was attributed to the absence of electron-withdrawing π-acid ligands in RuHClL$_2$. However, it was found that, to be isomerizable, an olefin needs a π-donor substituent (OR, NR$_2$, F). This is then a thermodynamic demand, because even the free carbene :C(X)R is stabilized by π-donor substituent X. This explains why hydrocarbon olefins are not isomerized to carbene complexes by RuHClL$_2$. Related transformations of unsaturated hydrocarbons have involved iridium,[14−17] osmium,[18] and ruthenium.[19]

We reasoned that a metal complex which was more π-basic than RuHClL$_2$ might convert olefins to an isomeric form which is more π-acidic. Our approach to such a complex was to go to a 5d metal (generally more "reducing" than a 4d metal), in a lower oxidation state than Ru(II). Our choice was rhenium, which already has some history as a source of enhanced reducing power.[20,21] In addition, there is evidence[22−24] that an amide, NR$_2$, is more *π-donating* than chloride, and thus we sought a rhenium complex with an amide ligand. Since amides are prone to β-H migration to make hydrido imine complexes,[25−29] it was attractive to have silicon as the substituent on N. This led us to attempt to install ligands of the sort pioneered by the Fryzuk group:[30−36]

† Present address: Department of Chemistry, Brandeis University, MS015, Waltham, MA 02454.

(1) Coalter, J. N.; Huffman, J. C.; Streib, W. E.; Caulton, K. G. *Inorg. Chem.* **2000**, *39*, 3757.
(2) Ferrando, G.; Coalter, J. N.; Gerard, H.; Huang, D.; Eisenstein, O.; Caulton, K. G. *New J. Chem.* **2003**, *27*, 1451.
(3) Ferrando-Miguel, G.; Gerard, H.; Eisenstein, O.; Caulton, K. G. *Inorg. Chem.* **2002**, *41*, 6440.
(4) Ferrando-Miguel, G.; Coalter, J. N.; Gerard, H.; Huffman, J. C.; Eisenstein, O.; Caulton, K. G. *New J. Chem.* **2002**, *26*, 687.
(5) Ferrando, G.; Gerard, H.; Spivak, G. J.; Coalter, J. N.; Huffman, J. C.; Eisenstein, O.; Caulton, K. G. *Inorg. Chem.* **2001**, *40*, 6610.
(6) Coalter, J. N.; Huffman, J. C.; Caulton, K. G. *Chem. Commun.* **2001**, 1158.
(7) Coalter, J. N.; Caulton, K. G. *New. J. Chem.* **2001**, *25*, 679.
(8) Caulton, K. G. *J. Organomet. Chem.* **2001**, *617*, 56.
(9) Coalter, J. N.; Bollinger, J. C.; Eisenstein, O.; Caulton, K. G. *New J. Chem.* **2000**, *24*, 925.
(10) Coalter, J. N.; Ferrando, G.; Caulton, K. G. *New J. Chem.* **2000**, *24*, 835.
(11) Coalter, J. N.; Huffman, J. C.; Caulton, K. G. *Organometallics* **2000**, *19*, 3569.
(12) Coalter, J. N., III; Streib, W. E.; Caulton, K. G. *Inorg. Chem.* **2000**, *39*, 3749.
(13) Coalter, J. N.; Bollinger, J. C.; Huffman, J. C.; Werner-Zwanziger, U.; Caulton, K. G.; Davidson, E. R.; Gerard, H.; Clot, E.; Eisenstein, O. *New J. Chem.* **2000**, *24*, 9.
(14) Crabtree, R. H.; Milhelcic, J. M.; Quirk, J. M. *J. Am. Chem. Soc.* **1979**, *101*, 7738.
(15) Kanzelberger, M. Singh, B.; Czerw, M.; Krogh-Jespersen, K.; Goldman, A. S. *J. Am. Chem. Soc.* **2000**, *122*, 11017.
(16) Krogh-Jesperson, K.; Czerw, M.; Summa, N.; Renkema, K. B.; Achord, P. D.; Goldman, A. S. *J. Am. Chem. Soc.* **2002**, *124*, 11404.
(17) Renkema, K. B.; Kissin, Y. V.; Goldman, A. S. *J. Am. Chem. Soc.* **2003**, *125*, 7770.
(18) Edwards, A. J.; Esteruelas, M. A.; Lahoz, F. J.; Lopez, A. M.; Onate, E.; Oro, L. A.; Tolosa, J. I. *Organometallics* **1997**, *16*, 1316.
(19) Borowski, A. F. Sabo-Etienne, S.; Christ, M. L.; Donnadieu, B.; Chaudret, B. *Organometallics* **1996**, *15*, 1427.
(20) Leeaphon, M.; Ondracek, A. L.; Thomas, R. J.; Fanwick, P. E.; Walton, R. A. *J. Am. Chem. Soc.* **1995**, *117*, 9715.
(21) Spaltenstein, E.; Erikson, T. K. G.; Critchlow, S. C.; Mayer, J. M. *J. Am. Chem. Soc.* **1989**, *111*, 617.
(22) Fryzuk, M. D.; MacNeil, P. A.; Rettig, S. J. *Organometallics* **1986**, *5*, 2469.
(23) Collman, J. P.; Sears, C. T. *Inorg. Chem.* **1968**, *7*, 27.
(24) Rahim, M.; Ahmed, K. J. *Inorg. Chem.* **1994**, *33*, 3003.
(25) Mayer, J. M.; Curtis, C. J.; Bercaw, J. E. *J. Am. Chem. Soc.* **1983**, *105*, 2651.
(26) Tsai, Y.-C.; Johnson, M. J. A.; Mindiola, D. J.; Cummins, C. C. *J. Am. Chem. Soc.* **1999**, *121*, 10426.
(27) Hartwig, J. F. *J. Am. Chem. Soc.* **1996**, *118*, 7010.
(28) Bryndza, H. E.; Tam, W. *Chem. Rev.* **1988**, *88*, 7010.
(29) Fryzuk, M. D. M., C. D. *Coord. Chem. Rev.* **1989**, *95*, 1.
(30) Fryzuk, M. D.; Giesbrecht, G. R.; Rettig, S. J. *Can. J. Chem.* **2000**, *78*, 1003.
(31) Fryzuk, M. D.; Leznoff, D. B.; Rettig, S. J.; Young, V. G., Jr. *J. Chem. Soc., Dalton Trans.* **1999**, 147.

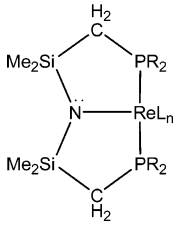

We communicated earlier on synthetic access to $(PNP^R)Re(H)_4$ and its reaction with ethylene.[37] We now report on the breadth and scope of this reaction with terminal and internal acyclic olefins, together with density functional theory (DFT) calculations designed to guide mechanistic analysis of these unusual and facile reactions. They indeed transform olefins in ways which are impossible for $RuHClL_2$.

Results

Installing the PNP^R Ligand on Re. We have previously reported[37] the synthesis of $(PNP^{Cy})ReOCl_2$ and its reduction under hydrogen atmosphere to $(PNP^{Cy})Re(H)_4$. Here we also report the preparation of analogous PNP$^{i\text{Pr}}$ and PNP$^{t\text{Bu}}$ compounds and the reactivity of these tetrahydrides with olefins. The preparation of the pincer ligands as their lithium salts was performed according to our modification of the original procedure by Fryzuk. These $(PNP^R)Li$ (**1**) derivatives were isolated and then converted to $(PNP^R)MgCl$ (**2**). We have previously reported[37] that the usage of PNP^{Cy} magnesium derivatives in the syntheses of $(PNP^{Cy})ReOCl_2$ resulted in superior yields compared to their lithium counterparts. $(PNP^{t\text{Bu}})MgCl$ (**2c**) can be conveniently isolated as its 1,4-dioxane adduct, but $(PNP^{i}Pr)MgCl$ (**2b**) can only be obtained as viscous oil and was therefore prepared in situ and used without isolation (Scheme 1).

Scheme 1

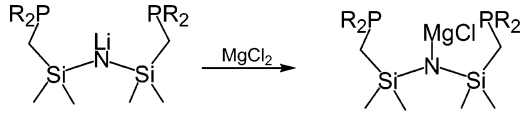

We were unsatisfied with the rather lengthy purification of $(PNP^{Cy})ReOCl_2$ synthesized from $(Ph_3PO)(Me_2S)ReOCl_3$. The preparation of compounds **4** can be substantially simplified by using $(Me_2S)_2ReOCl_3$ (**3**) as a starting material, which generates only inorganic salts ($MgCl_2$) or volatile Me_2S upon reaction with **2**. Additionally, its poor solubility, while not significantly retarding reactivity, permits easy separation of unreacted **3**. $(Me_2S)_2ReOCl_3$ was prepared via reduction of an HCl solution of $HReO_4$ by NaI in the presence of Me_2S (Scheme 2). Reduction of Re(VII) to Re(V) by iodide anion has been

Scheme 2

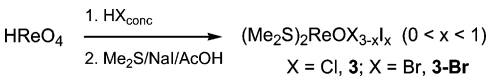

employed by Wilkinson in the synthesis of $(R_4N)_2ReOCl_5$.[38] The material was isolated in good yield and worked superbly in our syntheses of $(PNP^R)ReOCl_2$ (Scheme 3), although it may

Scheme 3

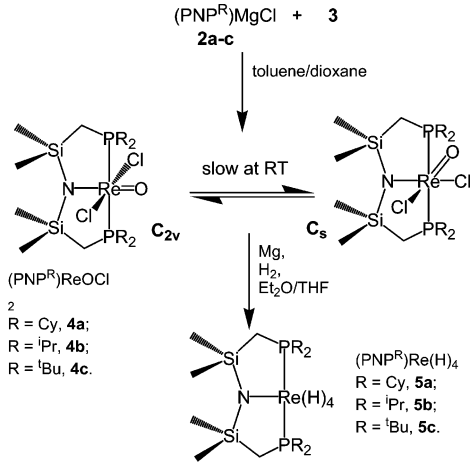

contain a small amount of iodide (see Experimental Section). We also prepared the bromide analogue of **3**, yellow-green **3-Br** (Scheme 2). **3-Br** served well as a Re starting material in the preparation of $(PNP^{Cy})ReOBr_2$.

The new Re complexes $(PNP^{i\text{Pr}})ReOCl_2$ and $(PNP^{t\text{Bu}})ReOCl_2$ have similar properties to the previously reported $(PNP^{Cy})ReOCl_2$. All three green compounds exist as mixtures of two isomers and are highly soluble in hydrocarbon solvents. Our previous report[39] detailed the thermal isomerization of $(PNP^{Cy})ReOCl_2$ (**4a**) into $(POP^{Cy})ReNCl_2$ (**6a**). The new complexes $(PNP^{i\text{Pr}})ReOCl_2$ (**4b**) and $(PNP^{t\text{Bu}})ReOCl_2$ (**4c**) undergo a similar transformation to form **6b** and **6c**, respectively. For the latter, this isomerization occurs at substantially lower temperatures. In fact, a small amount (5−10%) of $(POP^{t\text{Bu}})ReNCl_2$ (**6c**) is formed even during the time of synthesis and isolation of $(PNP^{t\text{Bu}})ReOCl_2$ (1−2 h at 22 °C). Solid samples of (**4c**) were stored in the freezer at −30 °C for months without change. For **4b**, the rate of this isomerization is approximately the same as for **4a**.

Installation of the Hydride Ligands. The tetrahydrides **5a**−**c** were prepared by Mg reduction of **4a**−**c** under H_2 atmosphere (Scheme 3). **5b** and **5c** are considerably more lipophilic than **5a** and therefore could only be recrystallized in good yield from solvents that, in our experience, are less solubilizing than pentane such as *neo*-hexane, tetramethylsilane, and hexamethyldisiloxane.

The NMR spectra of **5b**−**c** display the same key features as those of **5a**. The overall symmetry in solution is C_{2v}, and a single triplet of 4H intensity is observed at high field (t, $J_{H-P} = 22$ Hz, at −9.42 ppm for **5b**). At the same time, the aliphatic region of the ^1H NMR spectra of **5b**−**c** is considerably more useful than that of **5a**, for which it is essentially uninterpretable because

(32) Fryzuk, M. D.; Leznoff, D. B.; Thompson, R. C.; Rettig, S. J. *J. Am. Chem. Soc.* **1998**, *120*, 10126.
(33) Fryzuk, M. D.; Leznoff, D. B.; Ma, E. S. F.; Rettig, S. J.; Young, V. G., Jr. *Organometallics* **1998**, *17*, 2313.
(34) Fryzuk, M. D.; Gao, X.; Rettig, S. J. *Organometallics* **1995**, *14*, 4236.
(35) Fryzuk, M. D.; Gao, X.; Rettig, S. J. *J. Am. Chem. Soc.* **1995**, *117*, 3106.
(36) Fryzuk, M. D. Montgomery, C. D.; Rettig, S. J. *Organometallics* **1991**, *10*, 467.
(37) Ozerov, O. V.; Huffman, J. C.; Watson, L. A.; Caulton, K. G. *Organometallics* **2003**, *22*, 2539.
(38) Grove, D. E.; Wilkinson, G. *J. Chem. Soc. A* **1966**, 1224.
(39) Ozerov, O. V.; Gerard, H. F.; Watson, L. A.; Huffman, J. C.; Caulton, K. G. *Inorg. Chem.* **2002**, *41*, 5615.

of the multiple peaks arising from the Cy groups. Thus, **5b** shows a single methine signal and two signals belonging to the diastereotopic methyls of the isopropyl group in addition to one singlet (12H) arising from the Si−Me groups and one virtual triplet (4H) from the $SiCH_2P$ methylenes.

The reduction of **4a**−**c** by Mg must proceed in more than one step. NMR analysis of the reaction mixtures derived from **4a** at intermediate reaction times revealed (Scheme 4) the

Scheme 4

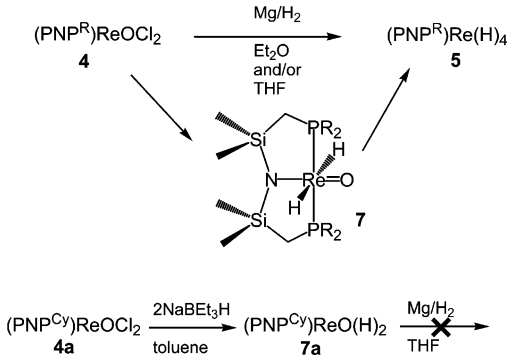

presence of $(PNP^{Cy})ReO(H)_2$ (**7a**), which completely disappears by the end of the reaction. Apparently, the removal of Cl ligands from Re occurs before the removal of the oxo group. The yellow complex **7a** was independently synthesized from **4a** and 2 equiv of $NaBEt_3H$ (Scheme 4). The NMR spectra are consistent with an average C_{2v} symmetry in solution, and the hydridic signal (2H) is observed as a triplet at 5.59 ppm. Such a downfield shift for a non-d^0 metal hydride is atypical, but in several reported complexes that contain hydrides cis to an oxo group, the hydrides resonate in the downfield region of the ^1H NMR spectrum. On the basis of this spectroscopic evidence, we propose the *mer*,*trans* structure for this compound. NMR resonances attributable to **7b** and **7c** were also observed at intermediate stages of the Mg/H_2 reductions of **4b** and **4c**. In contrast to **4**, **7a** is thermally stable (no change after 24 h at 90 °C in C_6D_6) and only a single isomer is observed. We believe that the *mer*,*cis*-isomer of **7** is thermodynamically disfavored because in such a structure a hydride ligand would be trans to the oxo ligand. The oxo ligand in **7** is the strongest trans influence ligand, and the preferred structure has the amido ligand (the weakest trans influence ligand) trans to it. The isomerization of **4** into **6** is a double silyl migration to O, and presumably requires the migrating silyl group to approach the oxygen atom.

While **7a** is an intermediate in the Mg/H_2 reduction of **4a**, pure samples of **7a** *failed* to react with Mg powder (same grade as used for the reduction of **4**) in THF or ether under 1 atm of H_2. We propose that the presence of $MgCl_2$ in solution is necessary for the reduction of the oxo group by Mg^0. In the Mg/H_2 reduction of **4**, 1 equiv of $MgCl_2$ is produced from the initial reduction of the Re−Cl bonds.

The tetrahydrides **5** are operationally unsaturated complexes in the sense that they can only achieve an 18e count by accepting π-donation from the amido N. Such π-donation, however, does not completely quench the electrophilic, unsaturated character of the Re center. Indeed, **5a** was found to readily form adducts with a number of 2e ligands (Scheme 5). This may be viewed as competition between the lone pair of N and an external ligand **L** for the empty orbital at Re. With all three compounds **5a**−**c**,

Scheme 5

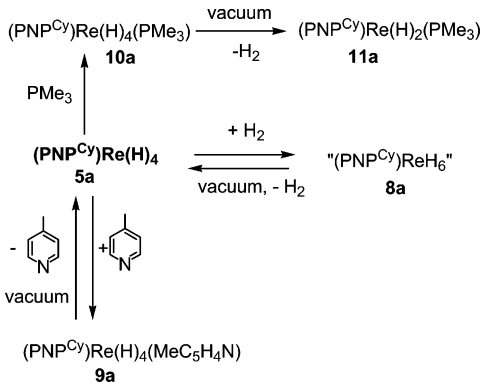

broadening of the hydride ^1H NMR signal and of the ^{31}P NMR signal is observed upon exposure to H_2, indicative of the reversible H_2 adduct formation. The analysis of the possible isomers of "$(PNP^{Cy})ReH_6$" (**8a**) by means of DFT calculations and by NMR has been reported.[37] In contrast, no change in the NMR spectrum of a C_6D_6 solution of **5c** is observed upon addition of 4-picoline. Evidently, the PNP^{tBu} ligand is too bulky to permit coordination of another ligand to Re in **5c**. Addition of 1 equiv of 4-picoline to C_6D_6 solutions of **5a** or **5b** causes broadening of the NMR resonances of both **5a**(**b**) and 4-picoline, as well as lightening of the purple-red color of **5**. Removal of the volatiles from these solutions regenerates pure **5a**−**b** quantitatively. The reaction of **5a** with 1 equiv of PMe_3, on the other hand, results in ca. 99% conversion to the colorless adduct $(PNP^{Cy})ReH_4(PMe_3)$ (**10a**), and exposure to vacuum results in the loss of H_2 (and not PMe_3) and formation of the blue-purple $(PNP^{Cy})Re(H)_2(PMe_3)$ (**11a**). Reactions with H_2, 4-picoline, and PMe_3 demonstrate the adaptability of the amido ligand which allows fast and reversible substrate binding.

The identity of **10a** was confirmed by a single-crystal X-ray study (vide infra). The quality of the X-ray data was sufficient to locate the hydrides and determine that **10a** is a classical tetrahydride. In the $^{31}P\{^1H\}$ NMR, a doublet is observed for the PNP phosphorus atoms (intensity of 2) and a triplet for the P of PMe_3 (intensity of 1). The overall apparent symmetry of the molecule at 22 °C according to the ^1H NMR is C_{2v}. The hydride signal is extremely broad at 20 °C (not observed). At −76 °C, the signal is decoalesced into three broadened resonances at −1.38, −2.20, and −9.30 ppm in 1:2:1 ratio. These NMR observations are thus consistent with the structure found by X-ray diffraction in the solid state (vide infra) where the two Re−H−(cis)H planes are approximately perpendicular. Such symmetry is also supported by DFT calculations on the model compound (vide infra).

The solution NMR data on **11a** are also consistent with the proposed formulation. A triplet (1P) and a doublet (2P) are observed in the ^{31}P NMR. The ^1H NMR data are consistent with the overall C_{2v} symmetry. The hydridic signal appears at −11.24 ppm as a doublet of triplets ($J_{HP(of\ PMe3)} = 75$ Hz, $J_{HP(of\ PNP)} = 11$ Hz). The 11 Hz coupling to the P atoms of the PNP ligand is typical for a hydride cis to a phosphine. The 75 Hz coupling to P of PMe_3 is rather unusual. It is well-known that the magnitude of the two-bond coupling constant between H and P (or P and P) attached to a metal center increases with the H−M−P angle increasing from 90° to 180°. Examples of complexes where the H−M−P angle is substantially smaller

Scheme 6

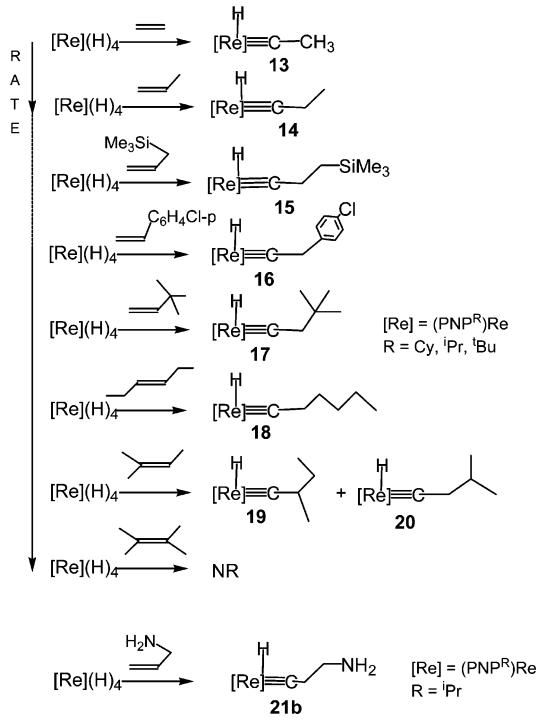

than 90° are quite rare. Rothwell reported[40,41] a series of Ta complexes **12** in which the H−Ta−P angle of ca. 65° results in a J_{HP} of 75 Hz, exactly the value we observe for **11a**. In the case of Rothwell's Ta d^0 hydrides the distortion away from the octahedral geometry was ascribed to the strengthening of the Ta−H bonds and of the π-bonding between Ta and the π-donor trans to PR_3. We believe that in **11a**, hydrides are similarly distorted away from N and toward PMe_3 and the diminished H−Re−P angle gives rise to an unusually high J_{HP}. The distortion of the hydrides in **11a** probably has the same origin as in **12**, serving to enhance the Re−H bonds and the Re−N bonding. Such distortion is also observed in **5**. In fact, **11a** can be viewed as a product of replacement of the two hydrides in the PNP plane in **5a** with a PMe_3 ligand.

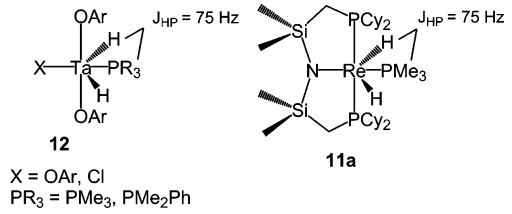

Notably, the conversion of **5a** to **11a** is a replacement of 2 H (lost as H_2) by a PMe_3 ligand achieved under very mild conditions. For most polyhydrides, replacement of 2H by PR_3 does not proceed readily and requires elevated temperature[42] and/or a sacrificial olefin to scavenge 1 equiv of H_2 by hydrogenation. The kinetic difficulty lies in the fact that polyhydrides of a general formula $(R_3P)_xMH_y$ are invariably saturated (18e) compounds and must react by a dissociative mechanism,

Table 1.[a]

R	13	14	15	16	17	18	19	20	21
Cy	**13a**	*n*	*n*	**16a**	**17a**	**18a**	**19a**	**20a**	*n*
^{i}Pr	**13b**	**14b**	**15b**	**16b**	**17b**	**18b**	*n*	*n*	**21b**
^{t}Bu	**13c**	*n*	*n*	**16c**	NR	NR	NR	NR	*n*

[a] NR = cannot be prepared according to Scheme 6. *n* = preparation not attempted. Numbers, e.g., **13a**, correspond to compounds that were observed or isolated.

whereas complexes **5** provide an easily accessible empty orbital and can react by an associative mechanism.

Reactivity of 5 with Acyclic Olefins. Our results on the reactivity of ethylene with **5a** have been communicated.[37] Here we report on extended studies including higher alkenes and **5b** and **5c** as well. In the presence of 4 or more equivalents of alkene, polyhydrides **5** are transformed into an equilibrium mixture of five-coordinate hydrido carbynes **13**−**20** and their six-coordinate olefin adducts **13***−**20*** (Schemes 6 and 7, Table

Scheme 7

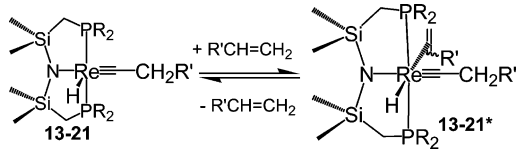

1). Qualitatively, the rate of the reaction is primarily governed by steric factors. For compounds **5a**,**b**, the reaction with even a stoichiometric amount of ethylene is complete in <5 min at ambient temperature; reactions with monosubstituted alkenes are also fast. Reactions with a 20-fold excess of 3-hexene proceed to completion in ca. 2 h at ambient temperature, while neither **5a** nor **5b** react with even neat C_2Me_4 at 110 °C. **5c** reacts much more slowly than **5a**,**b**, and the reaction proceeds only with ethylene and monosubstituted alkenes. For example, the reaction of **5c** with ethylene (1 atm C_2H_4) requires ca. 24 h to go to completion at ambient temperature, and the reaction of **5c** with 4-chlorostyrene requires ca. 10 h at 110 °C. **5c** does not react with larger alkenes even at 160 °C.

The solution NMR data for compounds **13**−**20** and **13***−**20*** are consistent with their formulation as rhenium carbynes. The carbyne carbons resonate in the 260−280 ppm region of the ^{13}C NMR spectrum and show J_{C-P} coupling of 11−12 Hz. The carbon chemical shift of the six-coordinate adducts is typically 10−20 ppm upfield of the five-coordinate hydrido carbynes. For compounds **13**−**20**, the hydride resonates (as a triplet) around −8 to −10 ppm. The hydride peak in **13b*** was found to be shifted downfield (2.21 ppm) compared to **13b**; a similar chemical shift was observed for the hydride in **16b*** (2.00 ppm). In five-coordinate carbynes, there is no ligand directly trans to the hydride, while in the six-coordinate adducts the hydride is trans to the coordinated alkene. It is well-known[43−47] that hydrides trans to an empty site generally display upfield chemical shifts. The ^{31}P NMR shows a singlet for **13**−**20** (except **19**), and selective decoupling of the alkyl hydrogens converts such singlets into doublets, showing hydride coupling.

(40) Clark, J. R.; Pulvirenti, A. L.; Fanwick, P. E.; Sigalas, M.; Eisenstein, O.; Rothwell, I. P. *Inorg. Chem.* **1997**, *36*, 3623.
(41) Parkin, B. C.; Clark, J. C.; Visciglio, V. M.; Fanwick, P. E.; Rothwell, I. P. *Organometallics* **1995**, *14*, 3002.
(42) Smith, K. J.; Ondracek, A. L.; Gruhn, N. E.; Lichtenberger, D. L.; Fanwick, P. E.; Walton, R. A. *Inorg. Chim. Acta* **2000**, *300*−*302*, 23.
(43) Esteruelas, M. A. W.; H. *J. Organomet. Chem.* **1986**, *303*, 221.
(44) Werner, H.; Wolf, J.; Hohn, A. J. *J. Organomet. Chem.* **1985**, *287*, 395.
(45) Intille, G. M. *Inorg. Chem.* **1979**, *11*, 695.
(46) James, B. R.; Preece, M.; Robinson, S. D. *Inorg. Chim. Acta* **1979**, *34*, L219.
(47) Masters, C.; Shaw, B. L. *J. Chem. Soc. A* **1971**, 3679.

The position of the equilibrium between a five-coordinate carbyne and its olefin adduct (Scheme 7) also depends primarily on steric factors. For derivatives of the PNP^{tBu} ligand, no detectable six-coordinate adduct was observed even in the case of ethylene. As we reported previously, for **13a** the equilibrium lies strongly on the side of the olefin adduct **13a***. The PNP^{iPr} analogue **13b** behaves similarly. The six-coordinate adducts of smaller monosubstituted olefins are observable in solution, but lose coordinated olefin readily upon exposure to vacuum at ambient temperature. The larger *neo*-hexene binds very weakly, causing only a broadening of the NMR resonances of the five-coordinate carbyne when present in large excess (ambient temperature). Alkene adducts were not observed for any di- or trisubstituted alkenes. Upon dissolution in C_6D_6 (ca. 22 °C), an equilibrium mixture of **16b**, **16b***, and 4-chlorostyrene is formed in the ratio of 1:10:1 (^{1}H and ^{31}P NMR integration). K_{eq} of 10 corresponds to ΔG of binding of 4-chlorostyrene of ca. 1.4 kcal/mol.

Alkene binding competes with π-donation from the amido lone pair for the empty orbital at Re. Similarly to the tetrahydrides **5**, five-coordinate carbynes **13**−**20** are also operationally unsaturated complexes. The color is very indicative: operationally unsaturated complexes tend to be deeply colored (carbynes, red; tetrahydrides **5**, purple-red) while classically saturated adducts are colorless (e.g., **10a**, **13***−**20***). Thus, dissolution of the colorless **16b*** leads to a reddish solution as a result of an equilibrium concentration of **16b**. The temperature-dependent nature of the equilibrium is evident from the gradual disappearance of color from solutions of **16b*** upon cooling and its reversible reappearance upon warmup.

The fact that hydrido carbynes were formed even from internal alkenes such as 3-hexene shows that, in some intermediate, the metal has the ability to migrate along the hydrocarbon chain to the terminus in order to form a carbyne product. The reaction of **5b** with excess (20 equiv) 3-hexene after 2 h at ambient temperature produces in situ a mixture of five-coordinate **18b** and two other products, each showing an AB pattern in the ^{31}P NMR spectrum in the 41−44 ppm region. Removing the volatiles in vacuo causes the AB ^{31}P signals to disappear, and the residue contains only **18b** (by NMR). Addition of excess 3-hexene to pure **18b** does not lead to changes observable by NMR. On the other hand, addition of 1-hexene to pure **18b** leads to the complete disappearance of the NMR signals of **18b** and the appearance of the two AB patterns observed in situ in the reaction of **5b** with 3-hexene. Removal of volatiles in vacuo regenerates pure **18b**. We conclude that these two pairs of AB patterns belong to the two possible diastereomers of a 1-hexene adduct of **18b** (**18b***, Scheme 7, R′ = *n*-Bu). Presumably, the alkene C−C bond is approximately aligned with the P−P vector in the six-coordinate adducts **13***−**20***, as was found (see below) in the solid-state structure of **13a***. This can lead to two diastereomers for monosubstituted alkenes: the substituent on the olefin is either syn or anti to the carbyne. In either of these isomers the phosphines are inequivalent, giving rise to AB patterns. Observation of only one such isomer for **16b*** (a pair of AB doublets, 36.5 and 41.7 ppm, J_{P-P} = 99 Hz) indicates a greater energy difference between the two diastereomers, likely because of the increased steric demand of an aryl substituent compared to an *n*-alkyl. The 1-hexene adducts **18a*** were also observed in the reaction of **5a** with 3-hexene.

With straight chain alkenes, either terminal or internal, there is only one possible carbyne to be formed, where the metal is attached to the terminus of the hydrocarbon chain. In branched alkenes, there may be inequivalent chain termini, and thus more than one carbyne can be formed. Indeed, in the case of the reaction of **5a** with 2-methylbutene, two carbyne products (**19a**, **20a**) were identified by NMR. **19a** must have C_1 symmetry as the β-carbon has four different substituents. This lack of symmetry is consistent with our observation of an AB pattern (50.1, 50.3 ppm) in the ^{31}P NMR spectrum for one of the carbynes formed from **5** and 2-methylbutene and of a dissymmetric picture in its ^{13}C NMR. The J_{P-P} coupling constant in **19a** is 205 Hz, consistent with the approximately trans geometry of the two phosphine arms. The ca. two times smaller value of J_{P-P} for the alkene adducts **16*** and **18*** probably reflects the compression of the P−Re−P angle as a consequence of accommodation of an alkene ligand. For instance, the P−Re−P angle in the solid-state structure of **17a** is ca. 167° (vide infra), while for the adduct of even the smallest alkene, **13*a**, it is only 157.5°. It is reasonable to expect that alkenes larger than ethylene such as 1-hexene in **18*** or 4-chlorostyrene in **16*** will cause an even greater compression of the P−Re−P angle.

The five-coordinate carbynes **13**−**20** are all either viscous oils or extremely lipophilic solids, which prevented isolation of most of them as analytically pure solids. We were able, however, to obtain analytically pure, crystalline samples of **17a**, including a crystal suitable for an X-ray diffraction study (vide infra). Compounds **13**−**20** are also quite thermally stable. No decomposition could be detected after thermolysis (110 °C, 24 h) in a *protio*-alkane or arene solvent for **13a**−**c**, **16a**−**c**, and **17a**−**b** (others were not tested). No noticeable H/D exchange with C_6D_6 occurs in solutions of **13**−**20** at ambient temperature on the time scale of 24 h. Prolonged heating of C_6D_6 solutions does result in some H/D exchange as evidenced by the decrease in intensity of the hydride signal and the PNP resonances as well as the change in multiplicity for the latter.

Reactivity of 5b with Allylamine. With allylamine as a substrate we found that the reaction eventually gives the carbyne product, as it does with hydrocarbyl alkenes. After 2 h at ambient temperature, the reaction of 4 equiv of allylamine with **5b** gave an essentially colorless mixture of two diastereomers of **21*b**. Application of vacuum to this solution caused reddening; however, when the volatiles were completely stripped, the residual solid was of an off-white color. This solid was poorly soluble in aliphatic hydrocarbons yet dissolved readily in C_6D_6, giving a red solution. Stripping of the volatiles generated a colorless solid again. The solution of this colorless solid displayed somewhat broad signals in ^{1}H, ^{13}C, and ^{31}P NMR, consistent with its formulation as **21b**. No free or bound allylamine was detected in the solution of this solid, and elemental analysis confirmed the formulation of this solid as **21b**. We propose that an equilibrium exists between a monomeric **21b** (red) and its dimer (or oligomer) in which the dangling amino group of the carbyne moiety serves as a ligand to another molecule of **21b** forming a (colorless) adduct. In solution, the equilibrium lies on the side of the monomer, but in the solid state the di- or oligomerization prevails, judging by the (absence of) color and the decreased solubility. Compound **21b** is indefinitely stable in solution at ambient temperature, but decomposes slowly to unidentified products when heated

Scheme 8

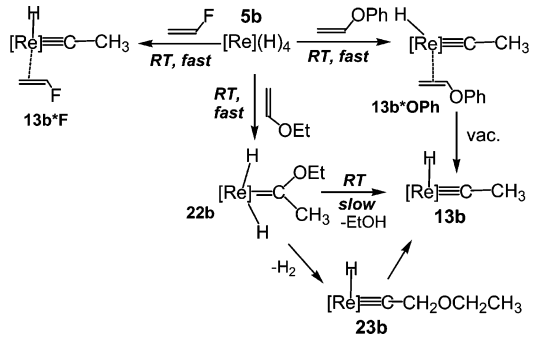

to 110 °C. The lower thermal stability of **21b** compared to **13**−**20** is probably caused by some degradation of **21b** by the amino functionality at elevated temperatures.

Reactivity of 5 with Heteroatom-Substituted Alkenes. Following the long standing interest in the transformations of heteroatom-substituted alkenes on strongly reducing transition-metal centers,[4,8] we also investigated the reactivity of **5** with such substrates. While the ambient temperature reactivity of allylamine parallels that of the simple hydrocarbyl alkenes, this was not found to be the case with vinyl ethers and vinyl fluoride. Addition of vinyl phenyl ether (4 or more equivalents) to solutions of **5b** in an arene or alkane solvent results, in the time of mixing, in the formation of a colorless solution. The ^{31}P NMR analysis of the resultant mixture revealed the presence of two sets of AB patterns. If this solution was allowed to stand for several hours, a significant amount of decomposition to unknown products was observed. The chemical shift and the J_{P-P} coupling constant for the observed pair of AB patterns were consistent with the formation of two diastereomers of a six-coordinate adduct of an alkene with a hydrido carbyne (**13b*OPh**, Scheme 8). Removal of the coordinated alkene in vacuo proceeded with difficulty to produce the red five-coordinate carbyne. The NMR resonances for this carbyne were consistent with it being **13b**. Thus, in the course of the reaction the C−O bond was cleaved. Addition of vinyl phenyl ether to an authentic sample of **13b** reproduced the ^{31}P NMR observation of two AB patterns. The difficulty in removing the alkene in vacuo is then simply explained by the low volatility of the alkene being removed: vinyl phenyl ether.

The reaction of vinyl fluoride with **5b** proceeded in a similar fashion to give a solution containing a major product (ca. 85%) displaying an AB pattern in ^{31}P NMR. Compared to the reaction with vinyl phenyl ether, the reaction with vinyl fluoride resulted in a slightly greater amount of decomposition products. Heating this product mixture in vacuo resulted in the disappearance of the AB pattern and the formation of **13b** as the major component (identified by ^{31}P, ^{13}C, ^{1}H NMR in situ), the product of C−F bond cleavage. This AB pattern corresponds to the major diastereomer of **13b*F**, the vinyl fluoride adduct of **13b**. Because of the low concentration of the minor isomer of **13b*F**, we were unable to identify its ^{31}P NMR resonances. However, the ^{19}F NMR signals of *both* isomers were identified, and the assignment was confirmed by observation of only these two ^{19}F NMR peaks when vinyl fluoride was introduced into a solution of an authentic sample of **13b**.

The reaction of **5b** with excess vinyl ethyl ether at ambient temperature proceeded rapidly to give, as the intermediate product, orange-red **22b** (Scheme 8). Concomitantly, Et_2O was produced (NMR evidence). Notably, neither EtF (^{19}F NMR) nor EtOPh (^{1}H NMR) were observed in the reactions of vinyl fluoride or vinyl phenoxide with **5b**. Unfortunately, the extreme lipophilicity of **22b** did not allow its isolation in a pure solid form, and it was characterized by solution NMR. At 22 °C, a ^{31}P{^{1}H} NMR singlet is observed, which changes to a broad triplet upon selective decoupling of alkyl hydrogens. In the ^{1}H NMR, a broad peak integrating to 2H at −9.89 ppm is observed, consistent with the presence of two H bound to Re. The other ^{1}H and ^{13}C signals at 22 °C are consistent with an average C_s symmetry. The signals corresponding to the EtO group are observed in the ^{1}H NMR, with the CH_2 group being considerably shifted downfield (4.31 ppm) from its position in Et_2O or EtOCH=CH_2. This shift may be indicative of substantial involvement of the oxygen in stabilizing the empty orbital of the carbene. In the ^{13}C NMR, the carbene α-C is observed as a triplet (J_{PC} = 8 Hz) at 273.1 ppm.

Since for a static **22b**, equivalence of *both* the P nuclei and the two Re−H does not seem possible, we undertook a low-temperature NMR study. At −60 °C, the two hydride signals are decoalesced into two well-separated broad peaks. At the same time, only one ^{31}P resonance is observed throughout the range of −60 to 22 °C, as well as only one set of EtO resonances in the ^{1}H NMR. There are several possibilities for the structure of **22b**. The carbene ligand may be either "in between" the two hydrides or "on the side" of them (**C** and **S**). For the structure **S**, it is also possible to have either a classical dihydride or a dihydrogen complex. It is unlikely that any minimum corresponds to the rotamer in which the plane of the carbene is in the plane of the PNP ligand because in that case we would expect to observe inequivalent ^{31}P nuclei. Both the (static) structures **C** and **S** should give rise to two inequivalent hydride signals. The rotation about the Re−C bond can serve to time-average the hydride signals at 22 °C in **C**. For **S**, the two hydrides may be exchanging by a rotation of an intermediate dihydrogen isomer. We currently favor structure **S** based on the DFT study of a model system (vide infra).

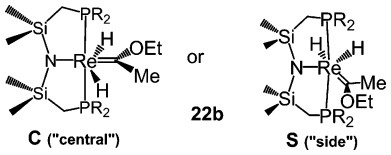

Thermolysis of **22b** (30 min, 80 °C) in the presence of ethyl vinyl ether produces five-coordinate **13b**, with some concomitant decomposition. The NMR signals of **13b** in the presence of an excess of ethyl vinyl ethers are only slightly broadened, indicating that ethyl vinyl ether binds to **13b** more weakly than vinyl phenoxide, vinyl fluoride, or other monosubstituted alkenes (vide supra). The conversion of **22b** to **13b** must proceed with loss of EtOH. Similarly, PhOH and HF are the expected coproducts in the reactions of **5b** with vinyl phenoxide and vinyl fluoride. The cleavage of Si−N bonds of the PNP ligand by ROH and HF could account for the partial decomposition observed in these reactions. To test this hypothesis, we conducted the reactions of Scheme 8 in the presence of a 20-fold excess of Me_3SiNMe_2 as a source of sacrificial Si−N bonds. In the case of vinyl ethers, solutions of **13b*OPh** and **13b** thus formed were >98% pure and persisted for at least 48 h without any sign of decomposition. The reaction of **5b** with vinyl

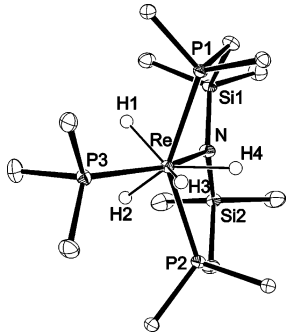

Figure 1. ORTEP drawing (PNP^{Cy})Re(H)$_4$(PMe_3) (**10a**) showing selected atom labeling. All hydrogen atoms not attached to Re and all methylene carbons of the Cy rings are omitted for clarity.

fluoride in the presence of a large excess of Me_3SiNMe_2 gave a substantially purer **13b*F**, although some side products were still observed. The observation of Me_3SiF by ^{19}F NMR in the latter reaction was crucial, supporting the proposed generation of HF.

Removal of volatiles in vacuo from solutions of pure **22b** results in partial conversion of **22b** to **13b** but also to **23b**. We propose the structure of **23b** based on the solution NMR evidence. The ^{31}P NMR singlet of **23b** resonates at ca. 61 ppm, in the region where signals of **13b**−**21b** are found. Selective decoupling of aliphatic hydrogens results in a doublet in the ^{31}P NMR spectrum, consistent with the presence of a single hydride on Re. Because **23b** was only observed as a minor component in the presence of other compounds, we were unable to obtain full ^1H and ^{13}C NMR data. However, the chemical shift and the value of J_{HP} (J_{CP}) for the ^1H hydride signal of **23b** and for the signal of the α-C were very similar to those of **13**−**21**. In addition, the signals arising from the two CH_2 groups connected to O in **23b** were also identified in the ^1H and ^{13}C NMR spectra.

23b was also observed when **5b** was allowed to react with 2 equiv of ethyl vinyl ether at 22 °C; after 2 h, the mixture consisted of (^{31}P NMR) **5b**, **13b**, **22b**, and **23b** in a 6:1:75:18 ratio. However, upon standing at 22 °C, the ratio changed to 11:19:69:1. Apparently under the reaction conditions, **23b** can be converted to **13b**, although at the present time the mechanism of this transformation is unclear.

Solid-State Structure of 10a (Figure 1, Table 2). A crystal of **10a** suitable for an X-ray diffraction study was obtained by treating a pentane solution of **5a** with excess PMe_3 and cooling the resultant solution to −30 °C. The quality of the X-ray diffraction data was sufficient to locate the hydride ligands, and these data show **10a** to be a classical tetrahydride. The Re center in **10a** is eight-coordinate, with the heavy atom donors forming a strongly flattened tetrahedral arrangement. The donor atoms are arranged in two approximately perpendicular planes: the first contains P1, P2, H1, H2 and bisects the H3−Re−H4 angle; the second contains P3, N, H3, H4 and bisects the H1−Re−H2 angle. The dodecahedral structure avoids placement of the strong trans influence hydrides trans to each other. The Re−P3 distance is somewhat shorter than the Re−P1 and Re−P2 distances, likely a consequence of the smaller cone angle of PMe_3. The key feature of the structure of **10a** is the long Re−N bond. Complex **10a** possesses an 18-electron count without the need for the π-donation from the amido N; therefore, the Re−N bond in **10a** is a single bond. This is in contrast to the structure[37]

Table 2. Selected Bond Distances and Angles in the Solid-State Structures of **10a** and **17a** (Two Independent Molecules)

	10a	**17a**, 1st molecule	**17a**, 2nd molecule
	Bond Distances, Å		
Re−N	2.2503(13)	2.112(3)	2.112(3)
Re−P1	2.4187(4)	2.3868(8)	2.3896(9)
Re−P2	2.4089(4)	2.3847(8)	2.3852(9)
Re−P3	2.3478(4)	−	−
Re−H1	1.55(3)	1.60	1.60
Re−H2	1.59(3)	−	−
Re−H3	1.60(3)	−	−
Re−H4	1.63(2)	−	−
Re−C31	−	1.761(3)	1.754(3)
N−Si1	1.6964(13)	1.737(3)	1.731(3)
N−Si2	1.6915(14)	1.722(3)	1.725(3)
H1−H2	1.88	−	−
H3−H4	1.77	−	−
	Bond Angles, deg		
P1−Re−P2	143.242(13)	167.34(3)	167.02(3)
N−Re−P3	153.36(4)	−	−
N−Re−C31	−	139.36(14)	139.66(14)
H1−Re−N		127.1	126.6
H1−Re−C31	−	92.3	93.7
Re−C31−C32	−	169.4(3)	171.0(3)

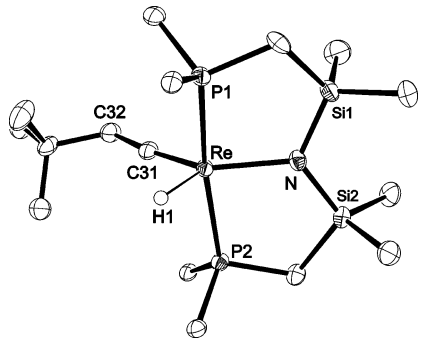

Figure 2. ORTEP drawing (PNP^{Cy})ReH(≡CCH_2CMe_3) (**17a**) showing selected atom labeling. All hydrogen atoms not attached to Re and all methylene carbons of the Cy rings are omitted for clarity.

of **5a** where the Re center can achieve the 18-electron configuration only by accepting π-donation from N. The Re−N bond in **5a** (ca. 2.06 Å) is much *shorter* than in **10a** (2.25 Å). At the same time, the average N−Si bond in **5a** (ca. 1.745 Å) is *longer* than in **10a** (ca. 1.694 Å) while the sum of angles about N is ca. 360° in both cases. The π-basic N of the PNP ligand is connected to three competing π-acids (Re and 2 Si). The longer Re−N bond in **10a** compared to **5a** is *not* simply a consequence of the higher coordination number of **10a**. In fact, the Re−P distances in **10a** are slightly shorter than those in **5a**.

Solid-State Structure of 17a (Figure 2, Table 2). The presence of a carbyne ligand is confirmed by the short Re−C bond comparable to other Re carbynes and by the near linear geometry of the Re−C31−C32 fragment. The coordination environment about the Re center in **17a** is most appropriately described as Y-shaped five-coordinate. The two phosphine donors are approximately trans to each other, while H1, N, and C31 form a Y-shaped geometry about the Re center in the perpendicular plane. The Y-shaped geometry is defined by an acute angle of 90° or less (here: H1−Re−C31) and two other angles of >120° (here: N−Re−C31, H1−Re−N). The overall geometry about Re is closely reproduced by the DFT calculation on the model compound **13^H**, including the position of the hydride ligand. The Y-shaped geometry can be understood as derived from a square pyramidal geometry with the π-donor

(here: N of PNP) shifting to a position that maximizes π-donation to the metal center.

We have previously reported[37] the structure of the six-coordinate **13a***, and now we report the structure of the five-coordinate, operationally unsaturated hydrido carbyne **17a**. We believe that the structure of **17a** is representative of the structures of **13**−**21**. The presence of the π-donation from N to Re in **17a**, but not in **13a***, is evinced by the much shorter Re−N bond in **17a** compared to that in **13a*** (ca. 2.28 Å) and the reverse trend in N−Si distances. Either of the structural comparisons between **5a** and **10a** or between **17a** and **13a*** is a comparison between an operationally unsaturated compound with a multiple, short Re−N bond and its saturated adduct with a long Re−N (single) bond.

Discussion

Transformations of Hydrocarbyl-Substituted Alkenes. The π-donating ability of the amido N contributes to the ability of the PNP^R ligand to sustain operationally unsaturated complexes. This is demonstrated by the facile and reversible binding of olefins by **13**−**20**,[37] of H_2 by **5** in the reactions of Scheme 5, and by the facile replacement of H_2 in **5** by PMe_3. Therefore, it is likely that the activation energy of binding of an olefin to **5** is quite small at ambient temperature. Hydrido carbyne complexes **13**−**21** contain the $(PNP^R)Re$ fragment and the elements of the corresponding alkene. It is clear then that, formally, the four hydrides of **5** are removed from, and the elements of the alkene added to, Re to give the hydrido carbyne product. The obvious proposal is that the four hydrides are spent in the hydrogenation of 2 equiv of alkene to the corresponding alkane. Thus, 3 equiv of alkene would be needed to produce a five-coordinate hydrido carbyne (**13**−**20**) from 1 equiv of **5**, and the fourth equivalent is necessary to produce an alkene adduct (**13***−**21***).

However, the reality is less straightforward. If an excess (20 equiv) of ^{t}BuCH═CH_2 is allowed to react with **5b** in a closed NMR tube in C_6D_6, then **17b** is produced quantitatively, but only 1 equiv (by ^{1}H NMR integration) of ^{t}BuCH_2CH_3 accompanies its formation. In another experiment, 3 equiv of *p*-chlorostyrene was reacted with 1 equiv of **5b** in a closed tube in *protio*-cyclohexane. After 2 h at ambient temperature, ^{31}P NMR indicated that the reaction mixture consisted of >90% **16b***, the remainder being the unreacted **5b** and the five-coordinate **16**. After 24 h at ambient temperature, the composition of this sample changed to contain ca. 50% of **16**, and after heating this mixture at 100 °C for 2 h, **16** became the dominant (>90%) component. Similar results were obtained in the reactions of allylamine with **5b**. With 2 equiv allylamine (closed tube), after 30 min at ambient temperature **21b** was the major (~90%) component and remained the major component after 48 h at 22 °C. If excess allylamine was allowed to react with **5b**, then **21b*** was the major product observed. These experiments indicate that under kinetic control only 2 equiv of alkene are needed to produce a five-coordinate hydrido carbyne, and 3 equiv to produce its six-coordinate alkene adduct. We propose that under *kinetic* control, two of the original four hydrides of **5** are released as free H_2. This H_2 can, over longer reaction times and/or higher temperature, hydrogenate another equivalent of alkene, but only *after* most of Re is converted to a hydrido carbyne (Scheme 9). Presumably, the barrier to hydrogenation

Scheme 9

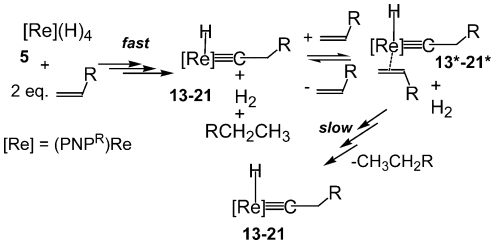

of **21b** by liberated H_2 is higher than for **16b** because H_2 has to compete with the pendant amino group for coordination to Re.

This reaction scheme implies that hydrogenation of a six-coordinate hydrido carbyne or even of a five-coordinate hydrido carbyne is slow. Indeed, exposure of a solution of **13a*** to 1 atm of H_2 (excess H_2, C_6D_6) does not lead to any immediate changes (by ^{1}H and ^{31}P NMR). Upon heating of this sample, it was found that **13a*** is completely converted to **5a** only after >10 h at 90 °C. When the five-coordinate **13a** was exposed to excess H_2, the complete hydrogenation to **5a** proceeded faster (10 h, 22 °C) than in the case of **13a***, but was still much slower than the time scale of formation of hydrido carbynes. Excess alkene suppresses the hydrogenation of the hydrido carbyne complexes because H_2 has to compete with alkene for coordination to Re.

The conversion of **5** to **13**−**21** is clearly a multistep transformation.[48−54] The proposed mechanism based on our observations and on literature precedents is outlined in Scheme 10. Initial coordination of alkene to **5** is followed by insertion into one of the Re−H bonds and reductive elimination of the corresponding alkane from **24**. Coordination of another alkene molecule may occur before or after alkane elimination from **24**, furnishing the alkene dihydride **25**. **25** can isomerize to the carbene dihydride **28**, which, with concomitant loss of H_2, evolves into the hydrido carbyne product (**13**−**21**).

We believe that the initial insertion is quite fast as demonstrated by an experiment with a relatively bulky alkene. When a heptane solution of **5b** was treated with 3 equiv of *cis*-stilbene (mp = −5 °C), a copious amount of *trans*-stilbene (mp = 122 °C) precipitated within ca. 2 min while still only and all of **5b** was observed in solution by ^{31}P NMR. The isomerization most likely proceeds by insertion/β-H-elimination. Reaction of *trans*-stilbene with **5b** proceeds only very slowly; at 100 °C, more than 24 h is required to consume **5b** by 3 equiv of *trans*-stilbene. Stilbene is not an olefin that can be isomerized to a hydrido carbyne, and thus this reaction yields a mixture of products (including bibenzyl) that apparently include products of activation of the solvent. The sluggishness of the hydrogenation of stilbene by **5b** should probably be attributed to its relative steric bulk (cf. Scheme 6). That may be an indication that reductive elimination from **24** is assisted by the incoming olefin.

(48) Shih, K.-Y.; Totland, K.; Seidel, S. W.; Schrock, R. R. *J. Am. Chem. Soc.* **1994**, *116*, 12103.
(49) Schrock, R. R.; Seidel, S. W.; Mosch-Zanetti, N. C.; Shih, K.-Y.; O'Donoghue, M. B.; Davis, W. M.; Reiff, W. M. *J. Am. Chem. Soc.* **1997**, *119*, 11876.
(50) Veige, A. S.; Wolczanski, P. T.; Lobkovsky, E. B. *Angew. Chem., Int. Ed.* **2001**, *40*, 3629.
(51) Freundlich, J. S.; Schrock, R. R.; Davis, W. M. *J. Am. Chem. Soc.* **1996**, *118*, 3643.
(52) Hughes, R. P.; Maddock, S. M.; Rheingold, A. L.; Guzei, I. A. *Polyhedron* **1998**, *17*, 1037.
(53) Miller, G. A.; Cooper, N. J. *J. Am. Chem. Soc.* **1985**, *107*, 709.
(54) Giannini, L.; Guillemot, G.; Solari, E.; Floriani, C.; Re, N.; Chiesi-Villa, A.; Rizzoli, C. *J. Am. Chem. Soc.* **1999**, *121*, 2797.

Scheme 10

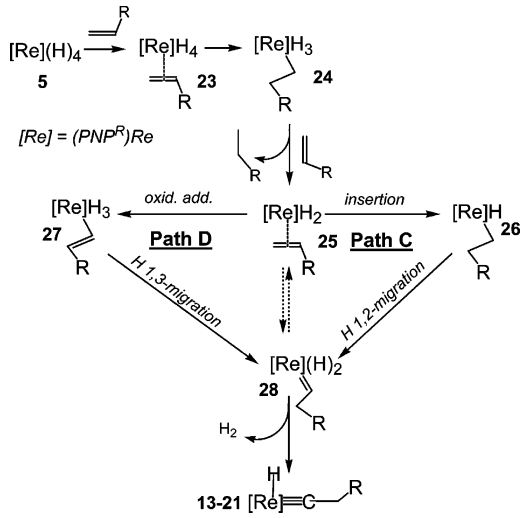

None of the species **26**−**28** were observed, but in certain cases we were able to observe analogues of **25** (Scheme 11). Allowing

Scheme 11

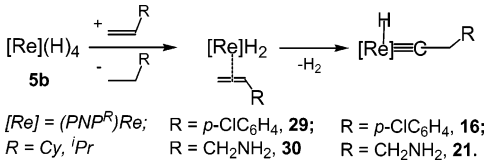

5b to react with 2 equiv of *p*-chlorostyrene in cyclohexane-h_{12} produces a mixture of **16b** and **5b** after 5 h. However, before this conversion is complete, a substantial amount of the species **29** was observed. **29** is characterized by an AB pattern in the ^{31}P NMR spectrum (J_{PP} = 92 Hz), and selective decoupling of the aliphatic hydrogens results in the splitting of each line in this AB system into a triplet. This is indicative of the presence of *two* hydrides on the Re center. No upfield ^{13}C resonance assignable to a carbene (such as in **28**) carbon was detected by ^{13}C NMR under conditions (concentration, time) where the carbene signal of **22b** or carbyne signals of **13**−**20** were unambiguously observed. These data are consistent with the proposed identity of **29**. Binding of a monosubstituted olefin will render the two ^{31}P nuclei in the molecule inequivalent regardless of the orientation of the olefin. We tentatively favor the structure of **29** where the C═C vector of the olefin is approximately aligned with the P−M−P vector based on the DFT studies of the model compound (vide infra). Because **29** is unstable in solution and transforms into **16**, we were unable to obtain it in a pure form in solution or in the solid state. Similar observations were made in the reaction of **5b** with allylamine. In addition to peaks of **21** and **21b***, the ^{31}P AB system (J = 178 Hz) of compound **30** was observed at shorter (<60 min) reaction times, which then transformed into **21b**. Compounds **29** and **30** were also observed (<1 h reaction time) in the reactions of **5b** with 3 equiv of *p*-chlorostyrene and allylamine (vide supra), respectively.

Isomerization of Internal Alkenes. The hydrido carbynes **18**−**20** are produced from internal alkenes. In the carbyne complexes, Re is attached to a terminus of the hydrocarbon skeleton, and thus the question arises of how Re migrates there from an internal position. Two possibilities can be envisioned (Scheme 12). If **25** and **28** (Scheme 10) can indeed interconvert

Scheme 12

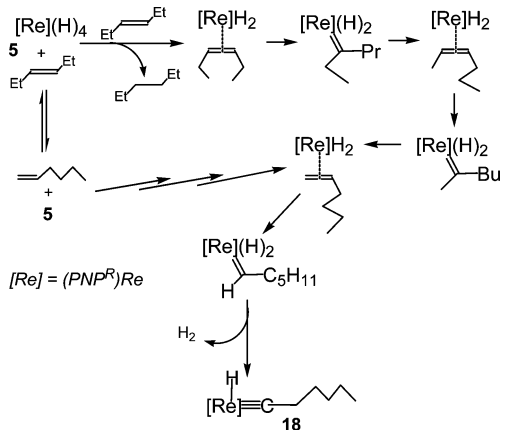

under the reaction conditions, then Re can traverse the skeleton without releasing free alkene. An alternative option is that **5** mediates fast isomerization of alkenes, thus producing an equilibrium concentration of *free* terminal alkene isomer, which is then transformed into the carbyne. The latter option is supported by the observation that the reaction of **5** with 3-hexene results in the formation of a mixture of **18** and **18***, i.e., some 1-hexene is generated beyond what may be needed to produce the carbyne. In addition, the potential of **5** for isomerizing alkenes is supported by the cis- to trans- isomerization of stilbene (vide supra). However, we cannot rule out that *both* pathways are operative.

Transformations of Heteroatom-Substituted Alkenes. Reactions of H_2C═CH−X (X = F, OPh, OEt) also lead to the hydrido carbyne products, thus testifying to the high preference of the (PNP^R)Re fragment for the formation of carbyne compounds. However, the difference from the reactions of hydrocarbyl-substituted olefins is that the C−X bond is cleaved in the process (Scheme 13), resulting only or primarily in

Scheme 13

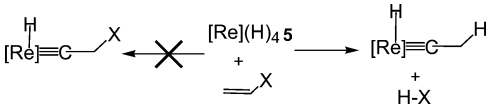

ethylidyne products.

In addition, we observed that the reactivity of H_2C═CH−OEt is different from the reactivity of H_2C═CH−OPh and H_2C═CH−F, as only in the case of ethyl vinyl ether did we see (vide supra) (a) the product of the hydrogenation of the double bond, (b) the observable and isolable alkoxycarbene intermediate **22**, and (c) the alkoxymethylcarbyne **23b** as a minor kinetic product. It seems reasonable to propose (Scheme 14) that initially coordination of H_2C═CH−X to **5** takes place, followed by insertion into a Re−H bond. Reductive elimination at this stage with formation of a C−H bond accounts for the formation of Et_2O (X = OEt). When X = F or OPh, reductive elimination from the β-X-substituted alkyl trihydride does not occur as Et-X is not observed for X = F, OPh. β-X-elimination followed by HX reductive elimination may be suggested as a competitive process. This would produce an ethylene complex which is then rearranged to hydrido ethylidyne as discussed

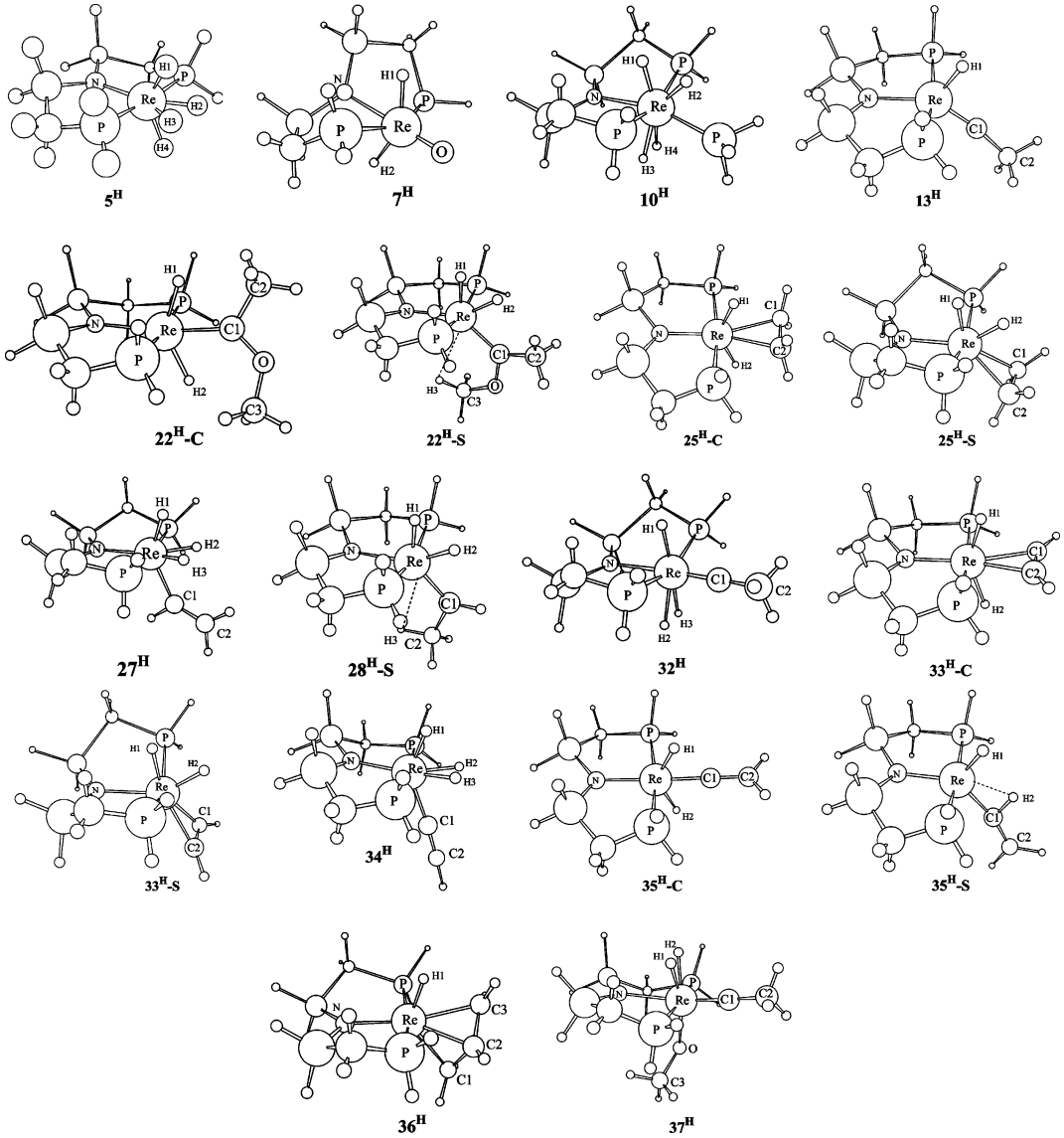

Figure 3.

Scheme 14

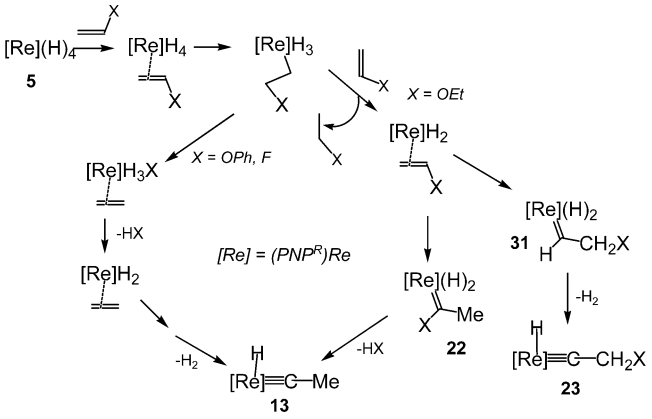

above. Since β-X-elimination implies migration of the X^- anion, OPh and F should be more prone to migrate than OEt. In the language of organic chemistry, OEt is a worse leaving (i.e., anion-forming) group than OPh or F.

It was previously shown[13] that vinyl ethyl ether can reversibly insert into the Ru−H bond of the $(^iPr_3P)_2$RuHCl fragment both in the 1,2 and 2,1 fashion. We propose here that the production of both **13b** and **23b** from **5b** and ethyl vinyl ether is a result of two competitive modes of insertion of ethyl vinyl ether into the Re−H bond of the $(PNP)ReH_2$ fragment. Insertion followed by α-H migration results in two different carbenes **22** and **31** (unobserved), which then produce **13** or **23** by loss of HX or H_2, respectively. Interestingly, all the transformations and intermediates shown in Scheme 14 are valid for X = H as well (cf. Scheme 10).

We have previously[2,3,5] described the chemistry of the cleavage of the C−X bond in vinyl-X compounds by $(R_3P)_2$-$Os(H)_3Cl$. The major final Os products for X = OPh or F (although not for X = OEt) were ethylidyne compounds $(R_3P)_2$-OsHClX(≡CMe), but in the case of X = F formation of ethylene from C_2H_3F was also observed. Intermediate carbene complexes $(R_3P)_2$OsHCl(=CMeX) were observed for X = OPh or OEt.

DFT Computational Evaluation of Potential Intermediates. Although we have not surveyed the entire PES for the carbyne synthesis reaction (in particular, we have not sought transition states), we have evaluated the free energies of several obvious *potential* intermediates. We used a model (H_2PCH_2-

Scheme 15

Scheme 16

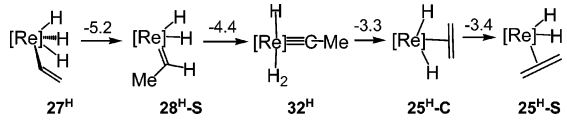

Scheme 17

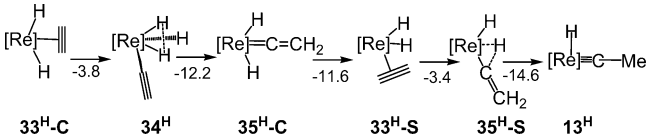

Scheme 18

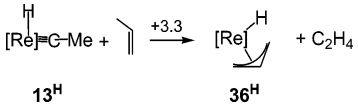

Scheme 19

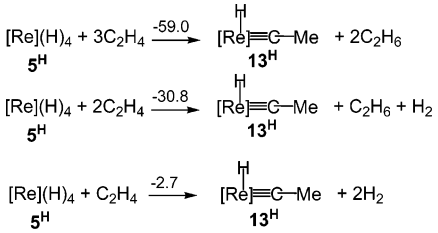

Scheme 20

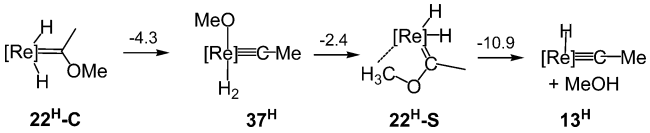

$SiH_2)_2N$ ligand (PNP^H) in our DFT (B3PW91) studies. Such model compounds will be denoted by the superscript "H". DFT is a vital supplement to experimental studies not only because it allows the strengthening of conclusions derived from experiment, but also because it can provide valuable information with respect to energetics of reactions.[55] It is also often indispensable as a source of information about energies and *geometries* of compounds not observed experimentally or some features of observed compounds evading experimental confirmation (e.g., hydride ligand positions). With that in mind, the two major objectives of our DFT study were to investigate the structures of the (PNP)Re complexes and to determine the relative energies of key compounds (and therefore the energetics of pertinent transformations). The structures of all the DFT-optimized geometries are pictured in Figure 3 and with energies given in Schemes 15−20 ($\Delta G°_{298}$ in kcal/mol).

Compound 7^H. The optimized structure of compound 7^H (trans,trans-isomer) can be described as a strongly distorted octahedron. The phosphine donors of the PNP ligand and the hydrides strongly bend away from the oxo ligand. Such bending away of ligands cis to an oxo (or nitrido) ligand has been attributed to the strengthening of the metal-oxo π-bonding. This is probably reinforced by the unfavorable nature of a 180° H−Re−H angle because of the high trans influence of the hydrides and by the chelate constraint that "pulls back" the phosphine arms. The Re−N(amido) distance of 2.345 Å is the longest among all molecules reported here. The oxo ligand should be regarded as a stronger π-donor than the disilylamido moiety of PNP. The 18e count at Re can be achieved by double-face π-donation from the oxo ligand, without need for the p-lone pair on N. The Re−N bond is thus a single bond. It is longer compared to other single Re−N bonds reported here, reflecting the high trans influence of the oxo ligand. The Re−O bond distance is very similar to that calculated[39] for $\mathbf{4^H}$.

Compound 10^H. The optimized structure of $\mathbf{10^H}$ reproduces the idealized mirror symmetry of the structure of **10a** obtained in the X-ray diffraction and solution VT NMR studies (1:2:1 hydride signals). However, the X-ray diffraction-derived structure of **10a** possesses four classical hydride ligands, whereas the DFT-optimized structure of $\mathbf{10^H}$ possesses one dihydrogen ligand (distance H3−H4 is 0.924 Å) and two hydrides (the structure with four hydride ligands is not a minimum on the potential energy surface). While it would be tempting to cite the unreliability of the X-ray diffraction for determination of exact hydride positions, we feel such a simplistic rationale *alone* is not sufficient. Besides the H−H distances, the DFT-optimized structure of $\mathbf{10^H}$ also possesses P1−Re−P2 and P3−Re−N angles that are larger than those in the X-ray diffraction structure of **10a**. It is consistent that to accommodate the increase in H−H distances (and thus in H−Re−H angles), the P1−Re−P2 and P3−Re−N angles should decrease. The origin of this discrepancy is not clear, but it is possible that it can be traced to use of the *model* PNP^H ligand (and PH_3 instead of PMe_3) in our DFT calculations. Compared to **10a**, $\mathbf{10^H}$ has seven out of nine alkyl substituents on the three phosphine donors replaced by hydrogens. This decreases the basicity of Re in the model system and therefore its ability to reduce η^2-H_2 to two hydrides. In addition, the steric bulk of the experimental ligand PNP^R may favor the arrangement of heavy atom donors about Re that is closer to tetrahedral (**10a**). The rehybridization of the Re d-orbitals as a consequence of such distortion may lead to higher stability of the dihydride structure (**10a**) vs the η^2-H_2 structure ($\mathbf{10^H}$). Whether a Re^{III} dihydrogen complex or a Re^V tetrahydride, **10** is an 18-electron complex without need for the p-lone pair of the amido N. Accordingly, the Re−N bond in $\mathbf{10^H}$ is calculated to be long at 2.210 Å, consistent with its single bond character. The near-zero free-energy change of eq 1 is, as discussed above:

$$[PNP]Re(H)_4 + PH_3 \xrightarrow[\text{kcal/mol}]{+1.2} [PNP]Re(H)_2(H_2)(PH_3) \quad (1)$$

consistent with considerable stabilization of the "operationally unsaturated" $[PNP]Re(H)_4$ by N → Re π-donation. Indeed, the calculated Re−N distance increases by 0.15 Å from reactant to product.

Compound 13^H. We chose $\mathbf{13^H}$ as a model for the five-coordinate hydrido carbynes **13**−**21**. The DFT-optimized geometry of $\mathbf{13^H}$ reproduces the key parameters of the experimentally determined structure of **17a** very closely. This agreement reinforces our confidence in the location of the hydride ligand in the X-ray diffraction study and in the overall Y-shaped geometry about Re.

(55) *Reactive Intermediate Chemistry*; Moss, R. A.; Platz, M. S.; Jones, M., Eds.; Wiley-Interscience: Hoboken, NJ, 2004.

Compound 32^H. We found that the hydrogenation of **13**−**21** to alkane and **5** is slow (and suppressed by alkene) and that the ^{1}H NMR spectrum of **13** exhibits only slight broadening of some peaks in the presence of H_2 (vide supra). These facts suggest that the binding of H_2 to **13**−**21** is weak, and this is confirmed in the DFT results. The calculated structure of $(PNP^H)ReH(\equiv CMe)(H_2)$ (**32^H**) is reminiscent of the X-ray structure[37] of **13a***, with the dihydrogen ligand in place of C_2H_4. The H−H distance of 0.88 Å is indicative of a very small amount of back-donation into the σ^* of H_2. The overall geometry about Re is approximately octahedral. The Re−C and Re−H(hydride) bond distances increase slightly compared to the structure of **13^H** while the Re−N bond is much longer (0.15 Å) in **32^H** compared to **13^H** due to loss of N → Re π-donation. The Re−N bond distance in **32^H** matches that in **13a*** quite closely. We calculate that the dissociation of H_2 from **32^H** is *exoergic* (Scheme 15). This is consistent with the lack of experimental observation of **32^H** at 22 °C.

Compound 22^H. We used DFT to investigate the possible isomers of carbene compound **22^H**. Since the observation of a ^{13}C resonance at 273.1 ppm in the spectrum of **22b** rules out the olefin π-complex formulation (i.e., $(PNP)ReH_2(\eta^2\text{-}H_2C{=}CHOEt)$) in favor of the carbene, we did not study the olefin complex isomers by DFT methods. The preference for a carbene (vs η^2-olefin) complex will generally be greater for heteroatom-substituted olefins.[8] Since the $(PNP)ReH_2$ fragment prefers the carbene isomer even for the cyclohexene/cyclohexylidene system,[56] we certainly expect unequivocal preference for a carbene in the case of vinyl ethers. We calculated the minimized geometries of the two isomers **C** ("central") and **S** ("side") for **22^H**. We find that the isomer **S** is lower in energy by 6.7 kcal/mol. Given the fact that experimentally we observe only one isomer of **22b** and that the **S** isomer is also preferred[56] for the related $(PNP)Re(H)_2(=C(CH_2)_5)$, it is reasonable to expect that the calculated preference for **22^H-S** is valid for **22b** as well. The Re−C distance is considerably shorter for **22^H-S** as compared to that of **22^H-C**. This indicates that the back-donation into the empty p-orbital of the carbene ligand is more effective when the carbene ligand is "on the side" of two hydrides than when it is "in between" the two hydrides. The diminished back-donation from Re in **22^H-C** is compensated by the increased π-donation from O as evidenced by the shorter C−O bond distance. Additionally, **22^H-S** possesses a short Re−H contact (2.610 Å) with one of the H's of the methoxy group. This weak agostic interaction may contribute to the overall preference for **22^H-S.** The DFT-optimized structure of **22^H-S** contains two classical hydrides. Discounting the agostic Re−H interaction, the Re center has a 16-electron valence count. The agostic interaction competes for the remaining empty orbital at Re with the p-lone pair of the amido ligand. The Re−N bond in **22^H-C** is shorter than that in **22^H-S.**

Compounds 25^H, 27^H, and 28^H. The optimized geometry of $(PNP^H)Re(H)_2(=CHMe)$ (**28^H**) is similar to that of **22^H-S** and $(PNP)Re(H)_2(=C(CH_2)_5)$. The ethylidene ligand shows an angular distortion at the α-C with the methyl group of the ethylidene bent toward Re, resulting in a close Re−H contact (2.729 Å). A similar distortion was observed in $(PNP)Re(H)_2(=C(CH_2)_5)$. The Re−N bond distance in **28^H** is intermediate between those in $(PNP)Re(H)_2(=C(CH_2)_5)$ and **22^H-S**. For **28^H** it can also be argued that the π-donation from N is in competition with the agostic interaction. The structure of **28^H** possesses two classical hydrides. $(PNP^H)Re(H)_2(\eta^2\text{-}C_2H_4)$ (**25^H**) and $(PNP^H)ReH_3(CH{=}CH_2)$ (**27^H**) are isomeric to **28^H**. We have obtained minimized energy geometries for two isomers of **25^H** where the C_2H_4 ligand is either between the two hydrides (**25^H-C**) or on the side of them (**25^H-S**). In both isomers, the C−C vector of the C_2H_4 ligand is oriented approximately parallel to the P−Re−P vector, i.e., perpendicular to the equatorial plane. Both structures are derived from a pentagonal bipyramid, and for a Re^{III} (d^4) center the two filled d-orbitals are orthogonal to the equatorial plane, thus the alignment of C_2H_4 is dictated by the symmetry match between the empty π^* orbital of C_2H_4 and the filled d-orbital of Re. Notably, the placement of the carbene ligands of **22^H** and **28^H** in the equatorial plane is also dictated by the symmetry of orbitals involved in back-donation. The Re−N bond is shorter in **25^H-C** than in **25^H-S**, similar to the corresponding isomers of **22^H** and **28^H** even though there are no agostic contacts in either isomer of **25^H**. This reaffirms that the Re−N π-interaction is stronger for "**C**" isomers of compounds of general formula $(PNP)Re(H)_2(L)$ even when in the "**S**" isomer there is no agostic CH donor competing with π-donation from N.

The minimized structure of **27^H** is similar to that of **5**, in which one of the hydrides is replaced by a vinyl group. However, in **27^H** the distance between the two hydrogens perpendicular to the PNP plane is shorter (1.349 Å) compared to those in **5^H**.

Compound **32^H** is also isomeric to **25^H**, **27^H**, and **28^H**. The relative free energies (kcal/mol) are presented in Scheme 16. The most stable isomer is calculated to be **25^H-S**, but, experimentally, only **13**, **13***, and **5** are observed as Re-containing products when **5** is allowed to react with <4 equiv of C_2H_4. The following reconciles the experimental observations with the DFT results: formation of **13^H** and free H_2 is endoergic by only 2.2 kcal/mol with respect to **25^H-S** and under experimental conditions of low H_2 concentration the equilibrium will be shifted toward loss of H_2 (and thus toward **13**). Formation of **13*** will further stabilize the carbyne product (ethylene binds to **13** more strongly than H_2). The model PNP^H ligand is much less sterically demanding than the experimentally used PNP^R ligands, and it should be expected that the experimental system should favor smaller steric profile ligands more so than the model DFT system. Therefore, we expect the DFT model to overestimate the stability of η^2-olefin isomers relative to carbenes and hydrido carbynes

If we look only at the relative η^2-ethylene/ethylidene stability, we find that **25^H-S** is more stable than **28^H-S** by 11.1 kcal/mol. This difference is larger than what we found for the cyclohexene/cyclohexylidene case and is perhaps too large to be overridden by the steric effect of the experimental PNP^R ligands. We find this consistent with the experimental observation of an olefin isomer for $(PNP^R)Re(H)_2(L)$ (L = olefin or isomeric carbene) in the case of **29** and **30** (monosubstituted olefins) and the carbene isomer for **32** (disubstituted olefin).

(56) Ozerov, O. V.; Watson, L. A.; Pink, M.; Caulton, K. G. *J. Am. Chem. Soc.* **2003**, *125*, 9604.

The spread of free energies for the isomers in Scheme 16 is only 16.3 kcal/mol. Given some uncertainty in the DFT numbers,[55] particularly as discussed above, the existence of these compounds cannot be ruled out as intermediates in the transformation of alkenes to hydrido carbynes on the basis of their thermodynamic stability.

Isomers of 13^H. We have also examined several structures isomeric to $\mathbf{13^H}$ to determine whether any obvious alternatives may be thermodynamically more stable than $\mathbf{13^H}$ but perhaps kinetically inaccessible. The relative free energies are presented in Scheme 17 (in kilocalories per mole). Clearly, $\mathbf{13^H}$ is the thermodynamically preferred isomer. The coordination environment about Re in compounds $\mathbf{33^H}$, $\mathbf{34^H}$, and $\mathbf{35^H}$ is similar to that in $\mathbf{25^H}$, $\mathbf{27^H}$, and $\mathbf{28^H}$, respectively, except for $\mathbf{35^H}$**-S**. $\mathbf{35^H}$**-S** is better described (Figure 3) not as a vinylidene dihydride but as a strongly α-agostic vinyl hydride, derived from the former by partial migration of H from Re to C. $\mathbf{34^H}$ possesses an η^2-H_2 (d_{HH} = 0.987 Å) ligand trans to N. This H−H bond shortens in the series of **5** → **27** → **34** as one of the hydrides in **5** is replaced by a vinyl (**27**) or ethynyl (**33**) group. Apparently the more electron-withdrawing vinyl and ethynyl cause the Re center to donate progressively less to the σ^* of H_2. The difference between the **C** and **S** isomers of $\mathbf{33^H}$ (27.6 kcal/mol) is much larger than that between the **C** and **S** isomers of $\mathbf{25^H}$ (3.4 kcal/mol). Unlike ethylene, acetylene can act as a four-electron donor, but it can only do so in the **S** isomer. This may account for the much larger energy difference. In addition, acetylene, as a stronger π-acid than ethylene, may be more sensitive to the degree of π-back-donation from Re in different isomeric structures. Indeed, the acetylene C−C bond is 0.056 Å longer in $\mathbf{33^H}$**-S** than that in $\mathbf{33^H}$**-C**, while for the two isomers of $\mathbf{25^H}$ the difference in the ethylene C−C bond distances is only 0.012 Å. For both $\mathbf{33^H}$ and $\mathbf{35^H}$, the Re−N bond is substantially shorter in the **C** isomer in accord with the above discussion.

Whereas the isomers in Scheme 16 consist of the elements of *ethane* plus the (PNP^H)Re fragment, the isomers in Scheme 17 consist of the elements of *ethylene* and the (PNP^H)Re fragment. Another possible isomer exists for alkenes higher than ethylene: the allyl hydride structure $\mathbf{36^H}$. To assess its thermodynamic stability, we have calculated the free energy of a hypothetical reaction (Scheme 18) between $\mathbf{13^H}$ and propene. From that we found that $\mathbf{36^H}$ is slightly endoergic with respect to $\mathbf{13^H}$. The preference for $\mathbf{13^H}$ is likely to be greater for the experimental PNP^R systems *and* for alkenes higher than propene because of steric factors.

Overall Reaction Free Energies. The reaction of 3 equiv of C_2H_4 with $\mathbf{5^H}$ to produce $\mathbf{13^H}$ and 2 equiv of C_2H_6 is calculated (Scheme 19) to be highly exoergic. However, our calculations indicate that the transformation of ethylene into a hydride and ethylidyne ligands is favorable even without concomitant hydrogenation of sacrificial double bonds (Scheme 19). This finding supports our observation that under kinetic control in the presence of excess alkene only 1 equiv of alkene is converted to alkane and 1 equiv of free H_2 is produced.

The free energy of binding H_2 to [PNP]ReH_2 is too large to make eq 2 a viable

$$[PNP]Re(H)_4 \xrightarrow{+15.0} [PNP]ReH_2 + H_2 \qquad (2)$$

mechanistic step at the temperatures employed here. However, the free energy of hydrogenation of ethylene, or any olefin, is sufficient to reverse this situation and thus furnish a reactive intermediate (e.g., [PNP]$Re(H)_2(C_2H_4)$). Although coordinated olefin is more stable than coordinated carbene, this deficit is overcome by elimination of H_2 and formation of the hydrido carbyne. Note also that H_2 is *not* bound to [PNP]ReH(≡CMe), consistent with the availability of H_2, in the reacting system, to hydrogenate olefin. The $\Delta G°_{298}$ for H_2 loss from [PNP]Re(H)(≡CMe)(H_2), −4.5 kcal/mol is dominated by a favorable entropy ($T\Delta S$ = 9.3 kcal/mol at 298K), since the dissociation enthalpy is only modest (+4.8 kcal/mol).[57]

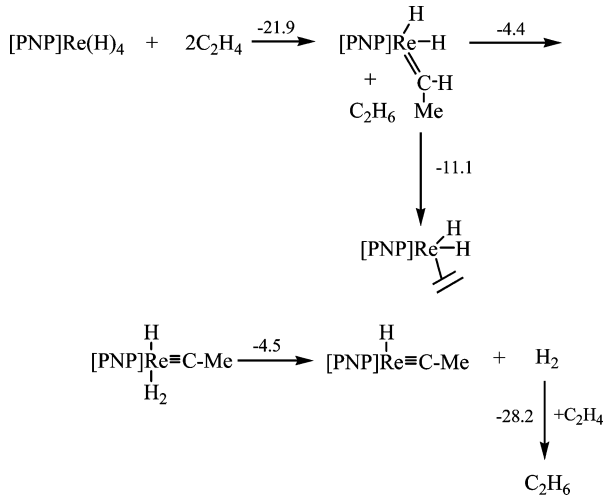

We have emphasized here how hydrogenation of added ethylene by [PNP]$Re(H)_4$ not only creates reactive intermediates, but enhances $\Delta G°_{298}$ for the creation of such intermediates, as well as of the final product. This is also illustrated as follows. Equation 3 shows the standard free energy

$$[PNP]Re(H)_4 + C_2H_6 \xrightarrow{+30.0} [PNP]ReH(H_2)(\equiv CMe) + 2H_2 \qquad (3)$$

$$C_2H_4 + H_2 \xrightarrow{-28.2} C_2H_6 \qquad (4)$$

for conversion of eth*ane* to a carbyne complex to be unfavorable. Only the addition of one or (better) two executions of "sacrificial" olefin hydrogenation (eq 4) could enable alk*ane* conversion to alkylidyne.

We also examined the formation of $\mathbf{13^H}$ from methyl vinyl ether (taken as a model for ethyl vinyl ether). We found elimination of MeOH from $\mathbf{22^H}$ to produce $\mathbf{13^H}$ to be preferred over the 1,2-shift of MeO to produce $\mathbf{37^H}$ (Scheme 20). Elimination of MeOH from $\mathbf{22^H}$ might also produce compounds isomeric to $\mathbf{13^H}$, but we have already shown here the thermodynamic preference for $\mathbf{13^H}$. Both ROH elimination and RO migration to the metal have been observed in related alkoxycarbene complexes of Os.[2,5]

Conclusion

[PNP]$Re(H)_4$ reacts with acyclic olefins under quite mild conditions, with hydrogen removal from Re, to leave behind lower valent reactive transients which act to strip H from additional olefin to convert it to hydride and carbyne ligands.

(57) Watson, L. A.; Eisenstein, O. *J. Chem. Educ.* **2002**, *79*, 1269.

Table 3. Calculated Distances for Figure 3

	Re–N	Re–C1	Re–C2	Re–C3	Re–H1	Re–H2	Re–H3	Re–H4	Re–PH_3	Re–O	H1–H2	H2–H3	H3–H4	C–O	C1–C2	C2–C3
5^H	2.062	–	–	–	1.639	1.664	1.664	1.645	–	–	–	–	1.525	–	–	–
7^H	2.345	–	–	–	1.673	1.673	–	–	–	1.694	–	–	–	–	–	–
10^H	2.210	–	–	–	1.665	1.668	1.791	1.791	2.347	–	1.607	–	0.921	–	–	–
13^H	2.123	1.756	–	–	1.649	–	–	–	–	–	–	–	–	–	1.469	–
22^H-C	2.066	2.059	–	–	1.637	1.639	–	–	–	–	–	–	–	1.341	1.519	–
22^H-S	2.123	1.987	–	3.046	1.627	1.654	2.610	–	–	–	–	–	–	1.354	1.503	–
25^H-C	2.021	2.309	2.309	–	1.651	1.658	–	–	–	–	–	–	–	–	1.414	–
25^H-S	2.110	2.203	2.203	–	1.630	1.651	–	–	–	–	–	–	–	–	1.426	–
27^H	2.068	2.046	–	–	1.650	1.667	1.667	–	–	–	–	1.349	–	–	1.336	–
28^H-S	2.147	1.903	2.820	–	1.633	1.652	2.729	–	–	–	–	–	–	–	1.514	–
32^H	2.274	1.763	–	–	1.681	1.822	1.822	–	–	–	–	0.880	–	–	2.117	–
33^H-C	2.004	2.238	2.238	–	1.680	1.689	–	–	–	–	–	–	–	–	1.259	–
33^H-S	2.131	2.013	2.013	–	1.702	1.657	–	–	–	–	–	–	–	–	1.315	–
34^H	2.017	2.034	–	–	1.669	1.732	1.732	–	–	–	–	0.987	–	–	1.226	–
35^H-C	2.077	1.937	–	–	1.638	1.643	–	–	–	–	–	–	–	–	1.312	–
35^H-S	2.013	1.930	–	–	1.657	1.978	–	–	–	–	–	–	–	–	1.334	–
36^H	2.030	2.178	2.244	2.378	1.648	–	–	–	–	–	–	–	–	–	1.437	1.402
37^H	2.281	1.762	–	–	1.723	1.718	–	–	–	2.040	0.998	–	–	1.390	1.465	–

The latter represent both greater formal electron donor number with regard to the 18-electron rule, but also greater π-acid character, which is more compatible with the high π-basicity of the electron rich [PNP]Re fragment. Reaction rates are predictably influenced by increasing substitution on the vinyl carbons, as is the formation constant for olefin binding to the product [PNP]ReH(≡CR). Heteroatoms F or OR on a vinyl carbon are cleaved under mild conditions, with liberation of HF or HOR; these can be scavenged to diminish degradation of the PNP ligand Si−N bonds. DFT calculations support and extend structural results from X-ray diffraction, but provide uniquely valuable energetic information on potential intermediates in these multistep transformations. There is abundant evidence from Re−N bond lengths, both experimental and computational, that the amide N in the PNP ligand can serve as a π-donor to stabilize otherwise unsaturated species. In addition, an examination of Tables 2 and 3 shows that the Si−N distance varies with the combined $\sigma + \pi$ basicity at N.

Experimental Section

General Considerations. All manipulations were performed using standard Schlenk techniques or in an argon-filled glovebox unless otherwise noted. All hydrocarbon reagents and solvents, Et_2O, THF, C_6D_6, C_7D_8, and C_6D_{12} were vacuum transferred or distilled from NaK/benzophenone/18-crown-6. PMe_3 and Me_3SiCl were vacuum-transferred and stored in the glovebox. Hexamethyldisiloxane was distilled from NaK alloy. Ethyl vinyl ether was distilled from CaH_2. Other reagents were used as received. The preparation of vinyl phenoxide in our labs has been described.[5] Compounds **1a**−**c**, **2c**, **5a**, **13a**, and **13a*** were prepared as reported elsewhere.[37] ^{1}H NMR chemical shifts are reported in ppm relative to protio impurities in the deuterated solvents. ^{31}P spectra are referenced to external standards of 85% H_3PO_4 (at 0 ppm). NMR spectra were recorded with a Varian Gemini 2000 (300 MHz ^{1}H; 121 MHz ^{31}P; 75 MHz ^{13}C), a Varian Unity Inova instrument (400 MHz ^{1}H; 162 MHz ^{31}P; 101 MHz ^{13}C), or a Varian Unity Inova instrument (500 MHz ^{1}H, 126 MHz ^{13}C). Usage of cyclohexane-d_{12} or protio solvents for NMR studies involving reactions of **5** with olefinic substrates was necessitated by the fact that noticeable incorporation of D into products occurred if C_6D_6 was used as solvent. Elemental analyses were performed by CALI, Inc. (Parsippany, NJ).

$(Me_2S)_2ReOCl_3$ (3). No precautions against introduction of air were taken during the synthesis of **3**. $HReO_4$ solution (5.0 g, 54 wt % Re, 14 mmol Re, Sandvik Chemicals) was treated with 25 mL of concentrated HCl and was stirred in a 200 mL flask. In a separate flask, NaI (4.5 g, 30 mmol) was dissolved in 50 mL of glacial acetic acid. Me_2S (2.55 mL, 35 mmol) was injected into the solution of NaI in AcOH, and it was briefly stirred with a glass rod. The resulting AcOH solution was added all at once to the HCl solution of $HReO_4$. Immediately, a copious amount of I_2 appeared in the flask. The flask was plugged with a rubber septum and stirred for 2 h at 22 °C. Then the suspension was poured onto a fritted glass funnel and filtered. The solids on the filter were washed with 2 × 5 mL of glacial AcOH, 3 × 10 mL of 5% HCl, 10 mL of glacial AcOH, and 2 × 5 mL of Et_2O. It was possible to wash away all of I_2 by extraction with AcOH or Et_2O, but this was unnecessary. The solids (mixture of **3** and I_2) were transferred to a Schlenk flask and were dried at 60 °C and 0.1 Torr for 24 h until all I_2 was sublimed off and then transferred into the glovebox. Yield: 4.6 g (76%). **3** decomposed when left in the air for several hours, as evidenced by blackening of the solid or when **3** came into contact with water or wet organic solvent. The decomposition was apparently insignificant in an acidic solution. According to the results of the elemental analysis, a small fraction of Cl in **3** ended up being replaced by I. However, we saw no evidence of incorporation of iodide into **4** when **3** was used as a starting material. Elemental Analysis. Found: C, 9.74; H, 2.26; Hal, 34.68. Calcd for $C_4H_{12}Cl_3OReS_2$: C, 11.10; H, 2.79; Hal, 24.57. Calcd for $C_4H_{12}Cl_{2.28}I_{0.72}OReS_2$: C, 9.63; H, 2.43; Hal, 34.53.

$(Me_2S)_2ReOBr_3$ (3-Br). 3-Br was prepared in a procedure identical to that of **3**, except using HBr instead of HCl. A yield of 0.91 g (57%) of yellowish-green **3-Br** was obtained starting from 1.0 g of $HReO_4$ (54 wt % Re, 2.8 mmol Re), 5 mL of concentrated HBr, NaI (0.90 g, 6.0 mmol), Me_2S (0.51 mL, 7.0 mmol), and 8 mL of AcOH.

$(PNP^{iPr})ReOCl_2$ (4b). (PNP^{iPr})Li (**1b**) (3.00 g, 7.10 mmol) was dissolved in 15 mL of THF, and $MgCl_2$ (0.86 g, 9.0 mmol) was added to it. This was vigorously stirred overnight, during which time the mixture became homogeneous. The resulting solution was poured into a flask containing a stirred suspension of $(Me_2S)_2ReOCl_3$ (**3**) in 50 mL of toluene/5 mL of 1,4-dioxane. The reaction mixture was stirred for 1 h, and then the volatiles were removed in vacuo. The residue was treated with 20 mL of heptane, stirred for 5 min, and then the volatiles were stripped again. The residue was extracted with pentane until the washings were near colorless. The deep green filtrate was stripped to ca. 20 mL and placed in the freezer at −30 °C for 24 h. The dark green, somewhat glutinous precipitate was separated from the supernatant by decantation, washed with cold pentane, and dried in vacuo to give 3.20 g (68%) of **4b** as a mixture of two isomers. Another 0.60 g (13%) of **4b** was obtained by an analogous procedure from the combined supernatant and pentane washings. Total yield: 3.80 g (81%).

The mer,cis-Isomer (Major). ^{1}H NMR (C_6D_6): δ 2.88 (m, J_{HH} = 7 Hz, 4H, PC*H*), 2.20 (m, J_{HH} = 7 Hz, 4H, PC*H*), 1.51 (apparent q (dvt), 8 Hz, 12H, PCH−CH_3), 1.20 (dvt, J_{HH} = 14 Hz, J_{HP} = 4 Hz,

2H, PCH_2Si), 1.18 (apparent q (dvt), 8 Hz, 12H, PCH−CH_3), 1.16 (apparent q (dvt), 8 Hz, 12H, PCH−CH_3), 0.63 (dvt, J_{HH} = 14 Hz, J_{HP} = 4 Hz, 2H, PCH_2Si), 0.56 (s, 6H, SiCH_3), 0.22 (s, 6H, SiCH_3). ^{31}P{^{1}H} NMR (C_6D_6): δ 8.4 (s). ^{13}C{^{1}H} NMR (C_6D_6): δ 27.6 (t, 14 Hz, P−*C*H), 25.7 (t, 11 Hz, P−*C*H), 18.8 (s, PCH−*C*H_3), 18.32 (s, PCH−*C*H_3), 18.27 (s, PCH−*C*H_3), 18.2 (s, PCH−*C*H_3), 12.2 (t, 5 Hz, PCH_2Si), 5.1 (t, 2 Hz, SiCH_3), 4.6 (br s, SiCH_3).

The mer,trans-Isomer (Minor). ^{1}H NMR (C_6D_6): δ 2.69 (m, J_{HH} = 7 Hz, 4H, PC*H*), 1.41 (t, J_{HP} = 4 Hz, 4H, PCH_2Si), 1.31 (apparent q (dvt), 8 Hz, 12H, PCH−CH_3), 1.20 (apparent q (dvt), 8 Hz, 12H, PCH−CH_3), 0.22 (s, 12H, SiCH_3). ^{31}P{^{1}H} NMR (C_6D_6): δ 16.7 (s). ^{13}C{^{1}H} NMR (C_6D_6): δ 26.7 (t, 11 Hz, P−*C*H), 19.0 (s, PCH−*C*H_3), 18.7 (s, PCH−*C*H_3), 11.9 (t, 4 Hz, PCH_2Si), 5.2 (t, 2 Hz, SiCH_3).

(PNP^{tBu})ReOCl$_2$ (4c). (PNP^{tBu})MgCl(dioxane) (**2c**) (3.38 g, 5.67 mmol) was added to a flask containing a stirred suspension of (Me_2S)$_2$ReOCl$_3$ (**3**) in 30 mL of benzene/5 mL of 1,4-dioxane. The reaction mixture was stirred for 1 h, and then the volatiles were removed in vacuo. The workup essentially identical to that of **4b** resulted in the combined yield (two fractions) of 3.08 g (75%). Only the mer,cis-isomer could be detected by NMR.

^{1}H NMR (C_6D_6): δ 1.46 (vt, 7 Hz, 18H, C*Me*$_3$), 1.34 (dvt, J_{HH} = 14 Hz, J_{HP} = 4 Hz, 2H, PCH_2Si), 1.24 (vt, 7 Hz, 18H, C*Me*$_3$), 0.61 (dvt, J_{HH} = 14 Hz, J_{HP} = 4 Hz, 2H, PCH_2Si), 0.59 (s, 6H, SiCH_3), 0.27 (s, 6H, SiCH_3). ^{31}P{^{1}H} NMR (C_6D_6): δ 6.7 (s).

(POP^{iPr})ReNCl$_2$ (6b). A sample of **4b** was heated in C_6D_6 for 5 h at 80 °C. Complete disappearance of **4b** was observed. The major component of the reaction mixture (>85%) was **6b**.

The mer,trans-Isomer (Major). ^{1}H NMR (C_6D_6): δ 2.94 (m, J_{HH} = 7 Hz, 4H, PC*H*), 1.51 (apparent q (dvt), 8 Hz, 12H, PCH−CH_3), 1.28 (t, J_{HP} = 4 Hz, 4H, PCH_2Si), 1.19 (apparent q (dvt), 8 Hz, 12H, PCH−CH_3), 0.09 (s, 12H, SiCH_3). ^{31}P{^{1}H} NMR (C_6D_6): δ 24.9 (s). ^{13}C{^{1}H} NMR (C_6D_6): δ 23.3 (t, 12 Hz, P−*C*H), 19.9 (s, PCH−*C*H_3), 18.3 (s, PCH−*C*H_3), 12.1 (t, 6 Hz, PCH_2Si), 2.7 (s, SiCH_3).

(POP^{tBu})ReNCl$_2$ (6c). A sample of **4c** was heated in C_6D_6 for 1 h at 80 °C. Full conversion to **6c** (mer,trans-isomer only) was observed by NMR.

^{1}H NMR (C_6D_6): δ 1.51 (vt, 7 Hz, 36H, C*Me*$_3$), 1.24 (vt, J_{HP} = 4 Hz, 4H, PCH_2Si), 0.24 (s, 12H, SiCH_3). ^{31}P{^{1}H} NMR (C_6D_6): δ 38.4 (s).

Syntheses of 5a−c. The Mg powder to be used was activated in a separate Schlenk flask by being stirred in a glovebox overnight in THF with Me_3SiCl (Si/Mg 0.02), and then the Mg powder was rinsed several times with THF to remove nonmetallic solids and dried in vacuo. A large excess (∼3 g) of Mg thus activated and a stir bar were placed into a 300-mL flask equipped with a Teflon vacuum valve and a SolvSeal (Andrews Glass) capped joint. In an Ar-filled glovebox (without stirring!) a precursor **4a−c** was added, along with 25−50 mL of Et_2O and ca. 20% $MgBr_2(Et_2O)$ (molar, per Re). The flask was taken out of the glovebox, and the contents were degassed by a freeze−pump−thaw cycle. Then the flask was allowed to warm to ca. −20 °C, back-filled with ∼ 1 atm H_2 using a gas line equipped with a manometer, and closed off. At this point vigorous stirring was initiated. With Mg activated as described here, the intense color of **5a−c** starts to appear within 15 min. H_2 was replenished at intervals. The reaction mixture may become slightly warm. The stirring was continued overnight, after which the volatiles were stripped to dryness. The residue was treated with heptane/dioxane and stripped, and then treated with heptane and stripped. The residue was then extracted with pentane and filtered, and the filtrate was stripped to dryness. This residue was dissolved in an appropriate solvent and filtered, and the product was obtained by crystallization at −30 °C, in two or more fractions, if necessary. **5a** was best crystallized out of pentane or a mixture of pentane with another alkane. **5b** and **5c** were best crystallized out of mixtures of *neo*-hexane with Me_4Si or $Me_3SiOSiMe_3$. The precipitates of **5b** and **5c**, after decantation of the supernatant, should be washed with cold Me_4Si followed by immediate drying in vacuo.

The flask used for the hydrogenation can be rinsed several times with THF until only Mg powder remains, and then the volatiles were removed in vacuo. The remaining Mg can be used repetitively for these experiments, even for complexes of different PNP ligands.

(PNP^{iPr})Re(H)$_4$ (5b). Isolated yield of 2.09 g (65%) from 3.70 g (5.56 mmol) of **4b**. ^{1}H NMR (C_6D_6): δ 1.90 (m, J_{HH} = 7 Hz, 4H, PC*H*), 1.16 (apparent q (dvt), 8 Hz, 12H, PCH−CH_3), 0.98 (apparent q (dvt), 8 Hz, 12H, PCH−CH_3), 0.75 (t, J_{HP} = 4 Hz, 4H, PCH_2Si), 0.32 (s, 12H, SiCH_3), −9.42 (t, 22 Hz, 4H, Re*H*). ^{31}P{^{1}H} NMR (C_6D_6): δ 66.5 (s). ^{13}C{^{1}H} NMR (C_6D_6): δ 31.5 (t, 14 Hz, P−*C*H), 19.2 (t, 2 Hz, PCH−*C*H_3), 18.3 (s, PCH−*C*H_3), 9.8 (s, PCH_2Si), 6.5 (t, 3 Hz, SiCH_3).

(PNP^{tBu})Re(H)$_4$ (5c). Isolated yield of 2.02 g (74%) from 3.08 g (4.30 mmol) of **4c**. ^{1}H NMR (C_6D_6): δ 1.29 (vt, 7 Hz, 36H, C*Me*$_3$), 0.98 (t, J_{HP} = 5 Hz, 4H, PCH_2Si), 0.35 (s, 12H, SiCH_3), −9.20 (t, 22 Hz, 4H, Re*H*). ^{31}P{^{1}H} NMR (C_6D_6): δ 83.6 (s). ^{13}C{^{1}H} NMR (C_6D_6): δ 37.8 (t, 10 Hz, P−*C*Me$_3$), 30.1 (s, PC*Me*$_3$), 10.2 (s, PCH_2Si), 6.4 (t, 2 Hz, SiCH_3). Elemental Analysis. Calcd (Found) for $C_{22}H_{56}NP_2ReSi_2$: C, 41.35 (41.40); H, 8.83 (9.48); N, 2.19 (2.18).

(PNP^{Cy})ReO(H)$_2$ (7a). (PNP^{Cy})ReOCl$_2$ (**4a**, 0.322 g, 0.390 mmol) was dissolved in 10 mL of C_6H_6. To this solution $NaBEt_3H$ in toluene (0.780 mL of 1.0 M solution, 0.780 mmol) was added. The color rapidly changed from green to brown. The reaction was stirred for 2 h at ambient temperature, and then the volatiles were removed in vacuo. The residue was treated with heptane, and the volatiles were stripped again. The residue was extracted with toluene and filtered. The filtrate was stripped, and the solids were washed with pentane and dried in vacuo to give 0.24 g (81%) of yellow **7a**.

^{1}H NMR (C_6D_6): δ 5.59 (t, 16 Hz, 2H, Re*H*), 2.22 (br t, 8H), 1.5−2.0 (several multiplets, 28H), 1.1−1.35 (several multiplets, 12H), 0.25 (s, 12H, SiCH_3). ^{31}P{^{1}H} NMR (C_6D_6): δ 35.6 (s). ^{13}C{^{1}H} NMR (C_6D_6): δ 37.7 (t, 12 Hz, P−*C*H), 29.5 (s, CH_2 of Cy), 29.3 (s, CH_2 of Cy), 27.5 (t, 5 Hz, CH_2 of Cy), 27.4 (t, 5 Hz, CH_2 of Cy), 26.7 (s, CH_2 of Cy), 20.1 (t, 4 Hz PCH_2Si), 3.1 (s, SiCH_3). Elemental Analysis. Calcd (Found) for $C_{30}H_{62}NOP_2ReSi_2$: C, 47.59 (47.59); H, 8.25 (8.48); N, 1.85 (1.58).

(PNP^{Cy})Re(H)$_4$(PMe$_3$) (10a). 5a (0.233 g, 0.300 mmol) was dissolved in 3 mL of pentane, and ca. 0.1 mL of PMe_3 was added to this solution. The solution became essentially colorless in the time of mixing. The solution was placed into a −30 °C freezer overnight. The next day the colorless crystalline (X-ray quality crystals) **10a** was isolated by decantation of the supernatant, washed with cold pentane, and blow-dried using a glass pipet inside the glovebox. Yield: 0.21 g (86%).

^{1}H NMR (C_7D_8, 20 °C): δ 2.12 (br s, 2H), 1.88 (br s, 12 H), 1.69 (br s, 12H), 1.42 (br s, 4H), 1.43 (dt, 8 Hz, 1 Hz, P*Me*$_3$), 1.27 (br m, 14 H), 0.88 (br t, 5 Hz, PCH_2Si), 0.39 (s, 12 H, Si*Me*). At 20 °C, the hydride signals were extremely broad and they could not be observed. ^{1}H NMR (C_7D_8, −76 °C, selected resonances, fine structure not completely resolved): δ −1.38 (br t, 28 Hz, 1H, Re-*H*), −2.20 (br dd, 28 Hz, 19 Hz, 2H, Re−*H*), −9.30 (br d, 72 Hz, 1H, Re−*H*). ^{31}P{^{1}H} NMR (C_6D_6, 22 °C): δ 33.1 (d, 15 Hz, 2P, PCy_2), −33.6 (br t, 1P, PMe_3). ^{31}P{^{1}H} NMR (C_7D_8, −76 °C): δ 33.5 (d, 15 Hz, 2P, PCy_2), −32.4 (t, 15 Hz, 1P, PMe_3). ^{13}C{^{1}H} NMR (C_7D_8, 20 °C): δ 37.8 (t, 10 Hz, P−*C*H), 30.7 (d, 36 Hz, P*Me*$_3$), 29.4 (s, CH_2 of Cy), 28.1 (s, CH_2 of Cy), 27.7 (two triplets overlapping, CH_2 of Cy), 27.2 (s, CH_2 of Cy), 17.3 (br s, PCH_2Si), 4.6 (s, SiCH_3).

(PNP^{Cy})Re(H)$_2$(PMe$_3$) (11a). 5a (0.467 g, 0.600 mmol) was dissolved in 10 mL of pentane, and ca. 0.1 mL of PMe_3 was added to this solution. The solution became essentially colorless in the time of mixing. Stripping the volatiles in vacuo produced mostly the colorless **10a** with some purple **11a**. This residue was heated at 120 °C under 0.1 Torr for 1 h and then redissolved in 5 mL of toluene, and the cycle was repeated twice more. NMR indicated complete conversion to **11a**. Analytically pure **11a** can be obtained by recrystallization from pentane at −30 °C. Yield: 0.410 g (84%).

^{1}H NMR (C_6D_6): δ 2.38 (br d, 48H), 1.75−1.88 (br m, 12H), 1.60−1.73 (multiplets, 8H), 1.58 (d, 6 Hz, 9H, P*Me*$_3$), 1.12−1.46 (multiplets, 20H), 0.79 (br t, 4H, PC*H*$_2$Si), 0.46 (s, 12H, SiC*H*$_3$), −11.24 (dt, 75 Hz, 11 Hz, 2H, Re*H*). ^{31}P{^{1}H} NMR (C_6D_6): δ 32.5 (d, 14 Hz, 2P, PCy$_2$), −66.5 (t, 14 Hz, 1P, PMe$_3$). ^{31}P NMR with selective decoupling of alkyl hydrogens showed a dt at 32.5 ppm and a tt at −66.5 ppm. ^{13}C{^{1}H} NMR (C_6D_6): δ 41.2 (t, 10 Hz, P−*C*H), 34.1 (d, 27 Hz, P*Me*$_3$), 30.3 (s, CH_2 of Cy), 29.3 (s, CH_2 of Cy), 27.9 (t, 4 Hz, CH_2 of Cy), 27.7 (t, 6 Hz, CH_2 of Cy), 27.2 (s, CH_2 of Cy), 13.0 (d, 4 Hz, P*C*H$_2$-Si), 7.2 (s, Si*C*H$_3$). Elemental Analysis. Calcd (Found) for $C_{33}H_{71}NP_3ReSi_2$: C, 48.50 (48.24); H, 8.76 (8.95); N, 1.71 (1.63).

(PNP^{iPr})ReH(≡C−CH$_3$) (13b) and (PNP^{iPr})ReH(≡C−CH$_3$)(C$_2$H$_4$) (13*b). (PNP^{iPr})ReH$_4$ (70 mg, 120 μmol) was dissolved in 2 mL of heptane in a Teflon-stoppered 50-mL glass vessel. The solution was degassed, and the vessel was filled with 1 atm of ethylene. The reaction yielded an essentially colorless solution in under 5 min. The volatiles were removed in vacuo at ambient temperature. The residue was dissolved in C_6D_6, and NMR indicated an essentially quantitative conversion to (PNP^{iPr})ReH(C−CH$_3$)(C$_2$H$_4$). The volatiles were removed in vacuo and the off-white residue was dried in vacuo at 160 °C for 30 min, during which time the color changed to the red of (PNP^{iPr})ReH(C−CH$_3$). This red oil was dissolved in Me$_3$SiOSiMe$_3$ (1 mL) and filtered through a pad of Celite to remove a minor amount of insoluble material. The filtrate was placed into a −30 °C freezer, and after 24 h the red crystalline product was separated by decantation and dried in vacuo. Yield: 45 mg (60%).

(PNP^{iPr})ReH(≡C−CH$_3$) (13b). ^{1}H NMR (C_6D_6): δ 2.09 (m, J_{HH} = 7 Hz, 2H, PC*H*), 1.83 (m, J_{HH} = 7 Hz, 2H, PC*H*), 1.23 (apparent q (dvt), 8 Hz, 6H, PCH−C*H*$_3$), 1.15 (apparent q (dvt), 8 Hz, 6H, PCH−C*H*$_3$), 1.14 (t, 3H, Re≡C−C*H*$_3$), 1.07 (apparent q (dvt), 8 Hz, 6H, PCH−C*H*$_3$), 1.04 (apparent q (dvt), 8 Hz, 6H, PCH−C*H*$_3$), 0.85 (AB dvt, J_{HH} = 14 Hz, J_{HP} = 4 Hz, 2H, PC*H*$_2$Si), 0.73 (AB dvt, J_{HH} = 14 Hz, J_{HP} = 4 Hz, 2H, PC*H*$_2$Si), 0.35 (s, 6H, SiC*H*$_3$), 0.30 (s, 6H, SiC*H*$_3$), −10.15 (t, 14 Hz, 1H, Re*H*). ^{31}P{^{1}H} NMR (C_6D_6): δ 61.09 (s). ^{13}C{^{1}H} NMR (C_6D_6): δ 271.5 (t, 11 Hz, Re≡*C*), 38.1 (s, Re≡C−*C*H$_3$), 29.6 (t, 12 Hz, P−*C*H), 29.0 (t, 11 Hz, P−*C*H), 20.0 (br s, PCH−*C*H$_3$), 19.0 (s, PCH−*C*H$_3$), 18.6 (s, PCH−*C*H$_3$), 17.6 (s, PCH−*C*H$_3$), 10.5 (s, P*C*H$_2$Si), 7.3 (s, Si*C*H$_3$), 6.3 (t, 2 Hz, Si*C*H$_3$).

(PNP^{iPr})ReH(≡C−CH$_3$)(C$_2$H$_4$) (13*b). ^{1}H NMR (C_6D_6): δ 2.39 (br d, 10 Hz, 2H, C_2H_4), 2.23 (m, J_{HH} = 7 Hz, 2H, PC*H*), 2.21 (t, 32 Hz, 1H, Re*H*), 2.13 (m, J_{HH} = 7 Hz, 2H, PC*H*), 1.48 (br m, 2H, C_2H_4), 1.31 (AB dvt, J_{HH} = 14 Hz, J_{HP} = 4 Hz, 2H, PC*H*$_2$Si), 1.30 (apparent q (dvt), 8 Hz, 6H, PCH−C*H*$_3$), 1.13−1.17 (three apparent q (dvt) overlapping, 18H, PCH−C*H*$_3$), 1.01 (t, 3H, Re≡C−C*H*$_3$), 0.98 (AB dvt, J_{HH} = 14 Hz, J_{HP} = 4 Hz, 2H, PC*H*$_2$Si), 0.21 (s, 6H, SiC*H*$_3$), 0.17 (s, 6H, SiC*H*$_3$). ^{1}H{^{31}P} NMR (C_6D_6, selected resonances): δ 2.39 (approximately d, 10 Hz, 2H, C_2H_4), 1.48 (approximately d, 10 Hz, 2H, C_2H_4), peaks at 2.39 and 1.48 ppm constitute an AA′XX′ system. ^{31}P{^{1}H} NMR (C_6D_6): δ 44.9 (s). ^{13}C{^{1}H} NMR (C_6D_6): δ 259.6 (t, 11 Hz, Re≡*C*), 37.8(s, Re≡C−*C*H$_3$), 32.7 (t, 11 Hz, P−*C*H), 30.4 (br s, C_2H_4), 29.3 (t, 15 Hz, P−*C*H), 20.6 (s, PCH−*C*H$_3$), 20.3 (s, PCH−*C*H$_3$), 20.2 (t, 5 Hz, P*C*H$_2$Si), 19.9 (s, PCH−*C*H$_3$), 18.8 (s, PCH−*C*H$_3$), 8.3 (t, 3 Hz, Si*C*H$_3$), 5.8 (br s, Si*C*H$_3$).

Experimental details for **13c−21b*** and **22b−30b** are given as Supporting Information.

(PNP^{iPr})ReH(≡C−CH$_3$)(H$_2$C═CH−OPh) (13b*OPh). 5b (30 mg, 52 μmol) was dissolved in 0.5 mL of *protio*-cyclohexane, and 0.1 mL of Me$_2$NSiMe$_3$ was added to this solution. No change was detected by ^{31}P NMR when this solution was allowed to stand for 1 day at ambient temperature. Vinyl phenoxide (19 μL, ca. 155 μmol) was added to this solution. The solution became colorless within minutes, and solids precipitated. Toluene (0.3 mL) was added to dissolve the precipitate, and a homogeneous solution resulted. ^{31}P NMR showed the presence of the two isomers of **13b*OPh**. The spectrum collected after this solution was allowed to stand for 10 days at ambient temperature showed no change. Removing the volatiles from this solution in vacuo results in formation of a mixture of **13b** and **13b*OPh**, but quantitative removal of the complexed vinyl phenoxide is difficult because of the low volatility of the free vinyl phenoxide. The two isomers of **13b*OPh** are exclusively observed (^{31}P NMR) when a solution of **13b** is treated with vinyl phenoxide.

Major isomer ^{31}P{^{1}H} NMR (toluene/cyclohexane/Me$_2$NSiMe$_3$): δ 46.5 (d, 110 Hz), 42.8 (d, 110 Hz).

Minor isomer ^{31}P{^{1}H} NMR (toluene/cyclohexane/Me$_2$NSiMe$_3$): δ 44.9 (d, 107 Hz), 43.2 (d, 107 Hz).

(PNP^{iPr})ReH(≡C−CH$_3$)(H$_2$C═CH−F) (13b*F). 5b (30 mg, 52 μmol) was dissolved in 0.5 mL of *protio*-cyclohexane, and 0.1 mL Me$_2$NSiMe$_3$ was added to this solution. The solution was degassed, and the NMR tube was back-filled with ca. 1 atm of vinyl fluoride. Within the time of mixing, the color changed to yellow-brown. ^{31}P NMR analysis showed that the major isomer of **13b*F** was the major (>85%) component of the mixture. ^{19}F NMR indicated the presence of a significant amount of Me$_3$SiF (−158.4 ppm). A few other minor peaks were observed. The volatiles were removed in vacuo, and the residue was dried at 100 °C and 0.1 Torr. The red color of **13b** developed, and it was confirmed as the predominant component of the mixture by ^{31}P, ^{1}H, and ^{13}C NMR (C_6D_6 solution). When solutions of **13b** were exposed to the atmosphere of C_2H_3F, only two ^{19}F peaks were observed. Both were also observed in the in situ reaction mixture above and we assigned them as the major and minor isomers of **13b*F**.

13b*F in *protio*-cyclohexane/Me$_2$NSiMe$_3$. Major isomer. ^{31}P{^{1}H} NMR: δ 44.7 (d, 111 Hz), 42.4 (d, 111 Hz). ^{19}F NMR: δ −170.8 (apparent dt, 68 Hz, 23 Hz). ^{1}H NMR (selected resonances, cyclohexane peak set to 1.40 ppm): δ 6.02 (ddd, J_{HF} = 68 Hz, Re(H$_2$C═C*H*F)).

Minor Isomer. ^{19}F NMR: δ −195.9 (doublet of multiplets, J_{HF} = 67 Hz).

Acknowledgment. This work was supported by the National Science Foundation.

Supporting Information Available: Full crystallographic narrative descriptions and data (CIF), computational methods and DFT calculated structures, together with experimental synthesis and spectra of compounds not in the main text (PDF). This material is available free of charge via the Internet at http://pubs.acs.org.

JA031617U